PERFORMANCE STUDY OF ASYNCHRONOUS/SYNCHRONOUS OPTICAL BURST/PACKET SWITCHING WITH PARTIAL WAVELENGTH CONVERSION

A THESIS

SUBMITTED TO THE DEPARTMENT OF ELECTRICAL AND

ELECTRONICS ENGINEERING

AND THE INSTITUTE OF ENGINEERING AND SCIENCES

OF BILKENT UNIVERSITY

IN PARTIAL FULFILLMENT OF THE REQUIREMENTS

FOR THE DEGREE OF

MASTER OF SCIENCE

By

Kaan Doğan

February 2006

I certify that I have read this thesis and that in my opinion it is fully adequate, in scope and in quality, as a thesis for the degree of Master of Science.

_____

Assoc. Prof. Dr. Nail Akar(Supervisor)

I certify that I have read this thesis and that in my opinion it is fully adequate, in scope and in quality, as a thesis for the degree of Master of Science.

_____

Assoc. Prof. Dr. Ezhan Karaşan

I certify that I have read this thesis and that in my opinion it is fully adequate, in scope and in quality, as a thesis for the degree of Master of Science.

_____

Assoc. Prof. Dr. Tuğrul Dayar

Approved for the Institute of Engineering and Sciences:

_____

Prof. Dr. Mehmet Baray
Director of Institute of Engineering and Sciences

ii

ABSTRACT

PERFORMANCE STUDY OF ASYNCHRONOUS/SYNCHRONOUS OPTICAL BURST/PACKET SWITCHING WITH PARTIAL WAVELENGTH CONVERSION

Kaan Doğan

M.S. in Electrical and Electronics Engineering

Supervisor: Assoc. Prof. Dr. Nail Akar

February 2006

Wavelength conversion is known to be one of the most effective methods for contention resolution in optical packet/burst switching networks. In this thesis, we study various optical switch architectures that employ partial wavelength conversion, as opposed to full wavelength conversion, in which a number of converters are statistically shared per input or output link. Blocking is inevitable in case contention cannot be resolved and the probability of packet blocking is key to performance studies surrounding optical packet switching systems. For asynchronous switching systems with per output link converter sharing, a robust and scalable Markovian queueing model has recently been proposed by Akar and Karasan for calculating blocking probabilities in case of Poisson traffic. One of the main contributions of this thesis is that this existing model has been extended to cover the more general case of a Markovian arrival process through which one can study the impact of traffic parameters on system performance. We further study the same problem but with the converters being of limited

range type. Although an analytical model is hard to build for this problem, we show through simulations that the so-called far conversion policy in which the optical packet is switched onto the farthest available wavelength in the tuning range, outperforms the other policies we studied. We point out the clustering effect in the use of wavelengths to explain this phenomenon. Finally, we study a synchronous optical packet switching architecture employing partial wavelength conversion at the input using the per input line converter sharing. For this architecture, we first obtain the optimal wavelength scheduler using integer linear programming and then we propose a number of heuristical scheduling algorithms. These algorithms are tested using simulations under symmetric and asymmetric traffic scenarios. Our results demonstrate that one can substantially reduce the costs of converters used in optical switching systems by using share per input link converter sharing without having to sacrifice much from the low blocking probabilities provided by full input wavelength conversion. Moreover, we show that the heuristic algorithm that we propose in this paper provides packet loss probabilities very close to those achievable using integer linear programming and is also easy to implement.

Keywords: Optical packet switching, optical burst switching, wavelength conversion, converter sharing, block-tridiagonal LU factorization, Markovian arrival process, wavelength scheduling

ÖZET

KISMİ DALGABOYU DÖNÜŞÜMLÜ EŞZAMANLI/EŞZAMANSIZ OPTİK ÇOĞUŞMA/PAKET ANAHTARLAMA PERFORMANS ANALİZİ

Kaan Doğan

Elektrik ve Elektronik Mühendisliği Bölümü Yüksek Lisans

Tez Yöneticisi: Doç. Dr. Nail Akar

Şubat 2006

Dalgaboyu dönüşümü optik paket/çoğuşma anahtarlamalı ağlarda çekişme çözürlüğünde en etkili yöntemlerden biri olarak bilinmektedir. Bu çalışmada, tam dalgaboyu dönüşümü yerine belirli sayıda dalgaboyu dönüştürücünün giriş veya çıkış bağlarında istatistiksel olarak paylaşıldığı kısmi dalgaboyu dönüşümünü kullanan çeşitli optik anahtar mimarilerini inceledik. Çekişmenin çözülememesi durumunda tıkanma kaçınılmazdır ve paket tıkanma olasılığı optik paket anahtarlamalı sistemleri inceleyen çalışmalarda önemli bir başarım ölçütüdür. Çıkış bağlarında dönüştürücü paylaşımlı eşzamansız anahtarlamalı sistemler için Akar ve Karaşan tarafından yakın zamanda sağlam ve ölçeklenebilir Markov kuyruk modeli önerilmiştir. Önerilen modelin trafik parametrelerinin sistem performansına etkisini incelemeye olanak sağlayan daha genel durum olan Markov varış süreçlerine genellenmesi bu tezin en önemli katkılarından biridir. Aynı sorunun kısıtlı erim dönüştürücüleri içeren türü de bu çalışmada incelenmiştir. Kısıtlı erim dönüştücücüleri sorunu için analitik bir model geliştirmek uygun olmadığı için, benzetim yolu ile optik paketin uygun olan en uzak dalgaboyuna

dönüştürüldüğü uzak dönüşüm yönetiminin incelediğimiz diğer yönetimlerden daha verimli olduğunu gösterdik. Ayrıca bu olguyu açıklamak için kullanımda olan dalgaboylarının öbeklenme etkisini vurguladık. Son olarak, giriş bağında kısmi dalgaboyu dönüşümünü sağlayan eşzamanlı optik paket anahtarlama mimarisini inceledik. Bu mimari için, doğrusal tamsayı programlama ile öncelikle en iyi dalgaboyu dönüşüm ayarlayıcıyı elde ettik ve sonrasında birkaç buluşsal algoritma önerdik. Bu algoritmalar benzetim yolu ile bakışımlı ve bakışımsız trafik senaryolarında denendi. Bu sonuçlar ile giriş bağlarında dalgaboyu dönüştürücü paylaşımı ile giriş bağlarında tam dalgaboyu dönüştürücü kullanımı ile elde edilen düşük tıkanma olasılıklarından çok taviz verilmeden dönüştürücü maliyetlerinde önemli miktarda kazanç sağlanabileceğini gösterdik. Buna ek olarak, önerdiğimiz buluşsal algoritmaların doğrusal tamsayı programlama ile elde edilen kayıp paket olasılıklarına çok yakın sonuçlar verdiğini ve kolay uygulanabilir olduğunu gösterdik.

Anahtar Kelimeler: optik paket anahtarlama, optik çoğuşma anahtarlama, dalgaboyu dönüşümü, dönüştürücü paylaşımı, Markov geliş süreci, dalgaboyu ayarlayıcı

ACKNOWLEDGMENTS

I gratefully thank my supervisor Assoc. Prof. Dr. Nail Akar for his guidance and endless patience throughout the development of this thesis.

Contents

List of Figures

List of Tables

Dedicated to my family and Fulya

Chapter 1

INTRODUCTION

Dramatic growth in Internet traffic demands has led to the use of Wavelength Division Multiplexing (WDM) systems which multiplex wavelengths of different frequencies onto a single fiber. This multiplexing operation creates multiple channels on the same fiber each carrying a different signal. Today's long-haul WDM systems support up to 160 channels each having a capacity of 10 Gb/s with an overall capacity of 1.6 Tb/s on a single fiber. On the other hand, client requirements are very diverse in terms of required capacity, connection utilization (continuous or bursty), connection duration, connection set-up times, etc. Using Optical Circuit Switching (OCS) at wavelenghth levels or simply circuit switching at subwavelength levels, today's wavelength-routed WDM networks route connection requests through the optical network to account for diversified capacity needs of users. In this switching paradigm, connection durations and set-up times tend to be very long and dynamic bandwidth sharing across clients is minimal which gives rise to inefficient bandwidth use especially for bursty data traffic. Its two-way reservation paradigm is considered to be another major deficiency since fiber cables are generally deployed over routes longer than 500km. Once the connection is set up, data remains in the optical domain throughout the lightpath, leading to a favorable transparent network architecture.

To cope with bursty traffic and for more efficient utilization of the fiber capacity, two new packet-based optical switching paradigms have been introduced: Optical Packet Switching (OPS) [1],[2] and Optical Burst Switching (OBS) [3],[4]. In optical packet switching, while the packet header is being processed either all-optically or electronically after an Optical/Electronic (O/E) conversion at each intermediate node, the data payload must wait in the fiber delay lines and be forwarded later to the next node. Thus, OPS requires line-rate header parsing and is thus viewed as a longer term solution due to the current technological limitations in packet header processing [2]. OBS, on the other hand, eliminates the need for header parsing by segregating the control and data planes. In OBS, the reservation request for a burst is signalled out of band by the use of a burst control packet which is processed in the electronic domain whereas the burst itself is transported end-to-end completely in the optical domain. When the control packet arrives at an optical burst switch towards its destination, the switch is configured for the corresponding data burst which would arrive after an offset time. Under the just enough time (JET) reservation protocol, allocated resources are released as soon as the burst is transmitted by the switch [3]. A comparison of the discussed switching paradigms is shown in 1.1. Although the control planes of OPS and OBS are different, both of them have similar data planes. Throughout this thesis, the terms "(optical) packet" and "(optical) packet switching" refer to a packet/burst and the data plane of OPS/OBS, respectively, since the analysis we pursue involves only the data plane of optical packet/burst switching.

Optical Switching Paradigm	Bandwidth Reservation	Contention	Optical Buffer	Challenging Issue
OCS	End-to-end	None	Not required	Coarse bandwidth
OPS	Link-by-link	Yes	Required	Large optical memory
OBS	Link-by-link	Yes	Not required	Blocking

Table 1.1: Comparison of three optical switching paradigms

In synchronous (i.e., time-slotted) optical packet switching networks, packet lengths are fixed and packets are assumed to arrive at slot boundaries. Such models are relatively difficult to implement due to the need for expensive synchronization equipment. In asynchronous (i.e., unslotted) networks, optical packet lengths are variable and packets arrive asynchronously and therefore there is not a need for costly synchronization equipment. On the down side, performance evaluation of asynchronous packet switching networks require advanced probabilistic methods and are generally more difficult.

One of the major issues in optical packet switching networks is *contention* which arises as a result of two or more incoming packets contending for the same output wavelength. Contention is resolved either in wavelength domain by wavelength converters, in time domain by Fiber Delay Lines (FDL), or in space domain by deflection routing [3]. If contention cannot be resolved by any one of the proposed techniques, then one or more contending packets will be blocked. Calculating the packet blocking probabilities is crucial in evaluating the performance of optical packet switching systems with a certain contention resolution capability set.

In this thesis, we first study the packet blocking probabilities for the "wavelength conversion" approach in which Tunable Wavelength Converters (TWC) are used for switching optical packets from any input wavelength into any output wavelength for contention resolution. In Full Wavelength Conversion (FWC), a packet arriving at a certain wavelength channel can be switched onto any other idle wavelength channel towards its destination. FWC reduces packet blocking probabilities significantly compared with the case of No Wavelength Conversion (NWC) [5],[6],[7]. However implementing all-optical FWC is very costly. Converter Sharing or in other words Partial Wavelength Conversion (PWC) is proposed as a cost-conscious alternative to FWC [8]. In PWC, there is a limited number of TWCs, and consequently some optical packets cannot be switched

towards their destination, i.e., blocked, when all converters are busy despite the availability of free wavelength channels on the output fiber. In PWC, TWCs may be configured as a single converter pool for converter sharing across all fiber lines, which is referred to as the Share-Per-Node (SPN) architecture [9]. A simpler architecture allows separate TWC banks per output fiber and the corresponding solution is called the Share-Per-Output-Line (SPOL) or simply SPL architecture [9] which is depicted in Fig. 1.1. Recently, a Share-Per-Input-Line (SPIL) architecture is proposed in [10] where a bank of TWCs is shared for all packets arriving on the same input fiber. SPN architecture has the best performance in terms of blocking, but requires complex add-drop multiplexer elements. Providing an exact analytical model for SPN does not appear to be feasible due to "curse of dimensionality" problem arising in such systems. The SPOL architecture leads to reduced switching costs but it has a relatively weak blocking performance.

Another separate issue in wavelength conversion is whether there is a specified range of wavelengths that a given wavelength can be converted to. Full Range TWCs (FR-TWC) do not have any tuning range limit and they can convert an incoming wavelength to any other wavelength. In limited-range wavelength conversion, a burst arriving on a wavelength can be converted to a fixed set of wavelengths above and below the original wavelength and such TWCs are called Limited-Range TWC (LR-TWC) [11]. The degree of conversion d is defined to be the total number of wavelengths available on both sides of the original wavelength and therefore an incoming optical packet can either be converted to one of the d destination wavelengths in the physical neighbourhood or can stay on the same wavelength if the latter is available.

We note that an analytical queueing model is proposed in [12] for the case of full-range SPOL-type partial wavelength conversion for asynchronous switching systems with Poisson packet traffic. As opposed to existing literature based on approximations and/or simulations, this model formulates the problem as
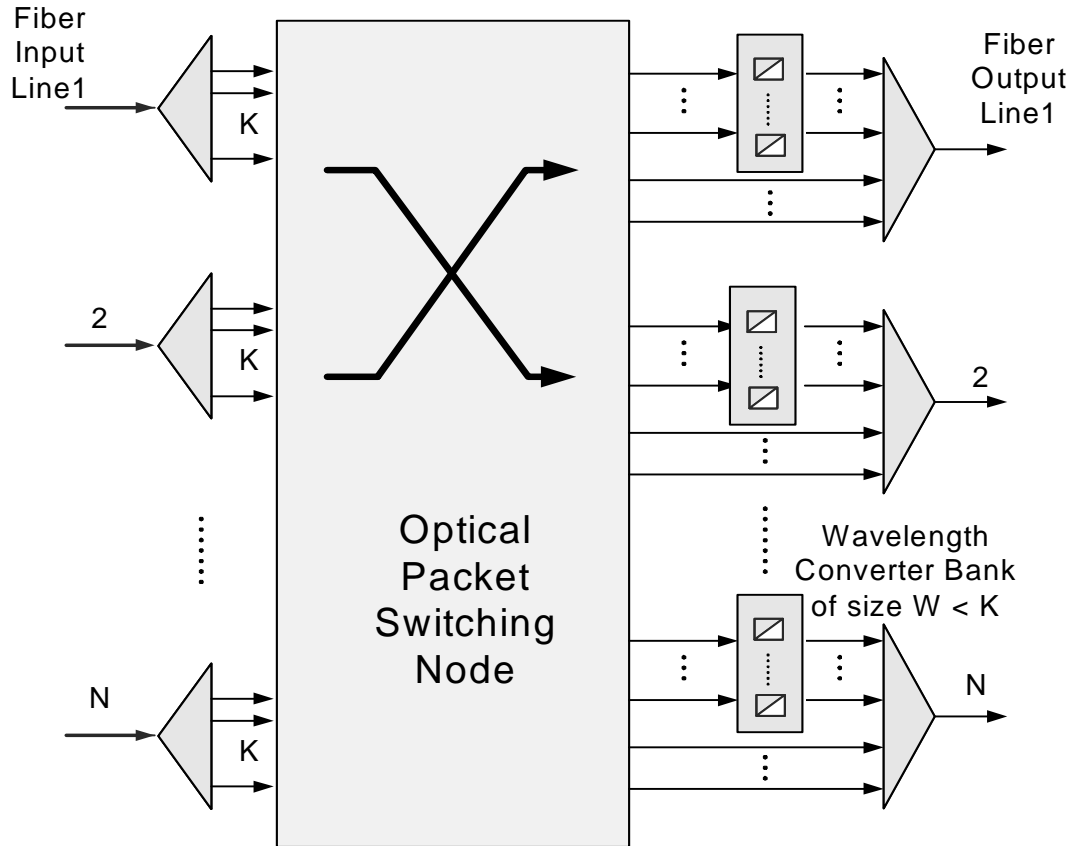
4

Figure 1.1: The general architecture of an optical packet switching node with N fiber I/O lines, K wavelength channels on each fiber line, and a bank of wavelength converters of size W shared per output line

one of finding the steady-state solution of a Continuous-Time Markov Chain (CTMC) with a block tridiagonal infinitesimal generator. A numerically efficient and stable solution technique based on block tridiagonal LU factorization was proposed and the authors showed that blocking probabilities can exactly and efficiently be found even for very large systems and rare blocking probabilities. One of the contributions of this thesis is that we generalize the model of [12] to more general packet arrivals that are modeled with the Markovian Arrival Process (MAP) that was first introduced in [13]; also see [14],[15],[16]. The MAP is a versatile process that allows correlation in packet interarrival times. Moreover, MAPs have a significant property that they are dense in the set of all stationary point processes. Special cases of the MAP are widely used in the literature for a variety of scenarios; the Interrupted Poisson Process (IPP) to approximate overflow traffic [17], a Phase Type (PH)-type process for fitting long-tailed data [18], a two-state Markov Modulated Poisson Process (MMPP) to describe the superposition of a number of on-off packet sources [19], more general MMPPs to model correlated aggregate Internet traffic [20],[21],[22]. We use the same technique used for Poisson arrivals this time for the case of MAP traffic and derive an expression for the blocking probabilities which gives us a way of studying the impact of traffic characteristics on the PWC-capable packet switch performance. With simulation studies, we investigate effect of packet length distribution on performance.

As a final contribution of this thesis, we study the performance of an asynchronous optical packet switch employing PWC on a share-per-link basis with the shared TWCs being of LR type. A similar analysis for the case of FR-TWCs in [12] does not seem to be plausible for the case of LR-TWCs due to the way conversion ranges overlap. Moreover, random conversion to any of the available wavelengths in the case of FR-TWCs provides the best results due to the uniform distribution of the incoming wavelengths. However, conversion policies substantially impact the performance for the case of LR-TWCs. The goal in this part

of thesis is to study different simple-to-implement wavelength conversion policies for the case of LR-TWCs. On the other hand, we give an approximate analytical procedure based on [12] to give a lower bound on the packet blocking probability with an auxiliary model that captures part of the complex system dynamics.

Finally, we investigate in this thesis two synchronous input wavelength conversion-based architectures that have been proposed and studied within the E-Photon-One Network of Excellence (NoE) project. We obtain closed-form expressions for blocking probabilities for the reference architectures and compare the architectures under symmetric and asymmetric traffic cases. We also propose an alternative architecture which employs sharing of wavelength converters at the input fiber lines. The proposed architecture brings the need for wavelength scheduling at the input section of the switch. We use an Integer Linear Programming (ILP) formulation for coping up with this scheduling problem and compare and contrast all the related switch architectures. We also propose different heuristical scheduling algorithms for online implementation since ILP solutions are not suitable for such implementations but rather used for performance benchmarking.

The rest of this thesis is organized as follows: In Chapter 2, we provide the Markovian analysis of PWC, compare the analytical results with simulation studies and finally generalize our results to the Markovian Arrival Process type packet arrivals. Chapter 3 addresses the conversion policies for LR-TWC's that are SPOL-type, identify "clustering effect" that significantly alters the blocking performance and provide a lower bound for the proposed policies. . In Chapter 4, we move on to input wavelength conversion,analyze a number of architectures and propose scheduling policies for better utilization of SPIL architecture. We conclude in Chapter 5.

Chapter 2

Full Range Tunable Wavelength Converter Sharing in Asynchronous Optical Packet Switching

In this thesis, we provide the blocking analysis of Optical Packet Switching link equipped with Full Range Tunable Wavelength Converters that are shared-per-output-link (SPOL).

We consider the online blocking model described in [23] in which lightpaths are set up and torn down at the packet level.

For the general PWC case, there is no closed form expression for the blocking probability and analytical results are also rare [24]. To the best of our knowledge, a numerical CTMC (Continuous Time Markov Chain) based algorithm for PWC in asynchronous SPL architectures is first proposed in [12]. Recently, a similar CTMC-based analysis is also proposed in [25] for the SPL case with Poisson packet arrivals and exponentially distributed packet lengths, and an approximate

analysis is proposed for the SPN case. Although the analysis of [25] for the SPL case is similar to that of [12], the block structure of the CTMC is not exploited and the authors report problems in large systems (e.g., $K = 64$) and for rare blocking probabilities. In [24], a fixed-point iteration-based approximate method for PWC for the SPN architecture is mentioned but not detailed. The work in [26] is simulation-based and attempts to find the number of wavelength converters required to attain a desired GoS (Grade of Service) in terms of blocking rates. In [9], simulations and an approximate analysis are provided for the same problem for the asynchronous case. Poisson and non-Poisson dynamic traffic patterns are simulated in [26] and [27] to show the impact of the packet arrival process on throughput. Simulation is generally a very useful tool since it can be applied to a wide range of models but i) simulations typically suffer from long run-times, ii) studying rare blocking probabilities may not be feasible, iii) it is computationally costly to use simulations in scenarios that might require iterations (e.g., analysis of networks, design and dimensioning problems, etc.).

2.1 Poisson Traffic

We study the asynchronous optical packet switch in Fig. 1.1 which has N input and output fiber lines and K wavelength channels per fiber. We assume a wavelength converter bank of size $0 \leq W \leq K$ dedicated to each output fiber. Optical packets destined to a particular output fiber line arrive at the switch from one of the N input fibers. We assume that the wavelength channel a packet arrives on is uniformly distributed on $(1, K)$, and packet durations are exponentially distributed with mean $1/\mu$.

A new optical packet arriving at the switch on wavelength w and destined to output line k

- is forwarded to output line k without using a TWC if channel w is available, else

- is forwarded to output line k using one of the free TWCs in the converter bank and using one of the free wavelength channels selected at random, else

- is blocked.

We concentrate only on one of the output fiber lines, say kth fiber, throughout this thesis and study its packet blocking performance. The overall switch performance can then be obtained using the individual output fiber blocking probabilities since we use complete TWC partitioning across output fiber lines. We first assume that the aggregate optical packet arrival process from the N input lines and destined for the output line k is Poisson with rate λ. This assumption is very common especially when N is large. For $W = K$ (i.e., full wavelength conversion), the OPS system behaves as an $M/M/c/c$ loss system with $c = K$ servers and offered load $q = \lambda/\mu$. On the other hand, the system load, or the traffic intensity is denoted by $\rho = q/c$ in an $M/M/c/c$ system which describes the offered work load to a single server [28]. For $W = 0$ (i.e, no wavelength conversion), we have K independent single server $M/M/1/1$ loss systems each with offered load $q = \lambda/\mu K$. In a general $M/M/c/c$ loss system, the blocking probability P_b can be obtained using the Erlang B formula [28]:

$$P_b = \frac{q^c/c!}{\sum_{i=0}^{c} q^i/i!} \tag{2.1}$$

A Markovian analysis for the partial wavelength conversion case, i.e., $0 < W < K$, is described below. Let $i(t)$ and $j(t)$ denote the number of wavelength channels and the number of TWCs that are in use at time t, respectively. The process $X(t) = \{(i(t), j(t)) : t \geq 0\}$ is a Markov process on the state space $S = \{(i,j) : 0 \leq i \leq K, 0 \leq j \leq min(i,W)\}$. To show this, let us assume that the process is in some state $(i,j), 0 \leq i < K, 0 \leq j \leq \min(i,W)$ at time t.

If a new packet arrives in the interval $(t, t + \delta t)$ which occurs with probability $\lambda \, \delta t + o(\delta t)$ (i.e., $\lim_{\delta t \to 0} o(\delta t)/\delta t = 0$) [29], then there are three possibilities:

a1) the wavelength on which the burst is riding is not currently used on the link which occurs with probability $(K - i)/K$ and the burst will be admitted and the process will jump to $(i + 1, j)$ at time $t + \delta t$,

a2) that wavelength is already used which occurs with probability i/K

    a21) then if $j = W$, then the packet will be blocked because the converter pool is all busy leading to no state change,

    a22) else if $j < W$, then the packet will be admitted on one of the available wavelengths randomly using one of the free converters and the process will make a transition to state $(i + 1, j + 1)$ at time $t + \delta t$.

When the process is in state (K, j) for some j at time t, then the arriving burst will be blocked since all wavelengths are busy.

Assume now that the process $X(t)$ is currently in some state $(i, j), 0 < i \le K, 0 \le j \le min(i, W)$ at time t. If a burst departs in the interval $(t, t + \delta t)$ which occurs with probability $i \mu \delta t + o(\delta t)$ then there are two possibilities:

b1) a TWC was used for this burst which occurs with probability j/i and the process $X(t)$ will jump to state $(i - 1, j - 1)$ at at time $t + \delta t$,

b2) a TWC was not used for this departing burst which occurs with probability $(i - j)/i$ and the process $X(t)$ will make a transition to state $(i - 1, j)$ at time $t + \delta t$.

When the process $X(t)$ is in state $(0, 0)$, then there cannot be any departures. It is thus clear that the process $X(t)$ is a CTMC.

The next step is to write the infinitesimal generator of this CTMC in a form that is amenable to numerically stable and efficient computation of the steady-state probabilities. For this purpose, we decompose the state space into subsets called levels such that the number of wavelengths in use is constant within a level and we enumerate the states in the following order:

$$S = \{ \underbrace{(0,0)}_{\text{level } 0}, \underbrace{(1,0),(1,1)}_{\text{level } 1}, \underbrace{(2,0),(2,1),(2,2)}_{\text{level } 2}, \cdots,$$
$$\underbrace{(K,0),(K,1),\cdots,(K,W)}_{\text{level } K} \} \tag{2.2}$$

Based on this enumeration, we conclude that state transitions can occur either among neighboring levels or within a level. The final step is to express the infinitesimal generator of the process $X(t)$ based on the observations a1, a21, a22, b1, and b2. For this purpose, we define the following three matrices for $i \geq 0$:

$$N_i = \begin{bmatrix} \frac{K-i}{K} & \frac{i}{K} & & & \\ & \frac{K-i}{K} & \frac{i}{K} & & \\ & & \frac{K-i}{K} & \ddots & \\ & & & \ddots & \end{bmatrix},$$

$$M_i = \begin{bmatrix} i & & & \\ 1 & i-1 & & \\ & 2 & i-2 & \\ & & \ddots & \ddots \end{bmatrix},$$

$$\bar{I}_i = \begin{bmatrix} 0 & 0 & \cdots & 0 \\ 0 & 0 & \cdots & 0 \\ \vdots & \vdots & \ddots & \vdots \\ 0 & 0 & \cdots & i/K \end{bmatrix}.$$

We also let I_i denote an identity matrix of size i. The process $X(t)$ is then written as a CTMC with a block-tridiagonal infinitesimal generator Q which is

in the following form:

$$Q = \begin{bmatrix} A_0 & U_1 & & & \\ D_0 & A_1 & U_2 & & \\ & D_1 & A_2 & \ddots & \\ & & \ddots & \ddots & U_K \\ & & & D_{K-1} & A_K \end{bmatrix}. \tag{2.3}$$

In the above generator, it is not difficult to show by using a1, a21, and a22 that

$$U_i = \lambda \bar{U}_i, \ \ 0 < i \le K \tag{2.4}$$

where $\bar{U}_{i+1}$ equals

$$\begin{cases} \text{upper-left } (W+1) \times (W+1) \text{ block of } N_i, & W \le i \\ \text{upper-left } (i+1) \times (i+2) \text{ block of } N_i, & 0 \le i < W \end{cases}$$

On the other hand, D_i in (2.3) is expressed as

$$D_i = \mu \bar{D}_i, \ \ 0 \le i < K \tag{2.5}$$

where $\bar{D}_{i-1}$ equals

$$\begin{cases} \text{upper-left } (W+1) \times (W+1) \text{ block of } M_i, & W < i \\ \text{upper-left } (i+1) \times i \text{ block of } M_i, & 1 \le i \le W \end{cases}$$

Finally,

$$A_i = \begin{cases} -(\lambda + i\mu)I_{i+1} & i < W, \\ -(\lambda + i\mu)I_{W+1} + \lambda \bar{I}_i & W \le i < K, \\ -i\mu I_{W+1} & i = K \end{cases} \tag{2.6}$$

Steady-state probabilities of this irreducible and aperiodic CTMC can be found by solving for the unique stationary solution [29]

$$xQ = 0, \ \ xe = 1 \tag{2.7}$$

where e is a column vector of ones of suitable size. Note that the size of Q is $(W+1)(K - \frac{W}{2} + 1)$ and calculating the stationary solution using conventional

13

finite Markov chain solution methods (see for example [30]) would be prohibitive especially for large systems, e.g., $K = 256$, $W >> 1$. Next we give a numerical solution procedure by taking advantage of the block-tridiagonal structure of the generator.

Since one of the equations in (2.7) is redundant, we can replace one of the equations, say the first equation in (2.7), by all ones to obtain a nonsingular system. For this purpose, let P be obtained by replacing the entries of the first column of Q with unity by setting

$$A_0 := 1, D_0 := \begin{bmatrix} 1 \\ 1 \end{bmatrix} \qquad (2.8)$$

Also let b be a zero row vector except its first unity entry. It is clear that if z is a solution to

$$zP = b \qquad (2.9)$$

then

$$x := \frac{z}{ze} \qquad (2.10)$$

gives the steady-state probabilities.

We propose the block tridiagonal LU factorization algorithm given in [31] for solving $zP = b$. In this algorithm, the goal is to obtain a block LU factorization of the matrix P:

$$P = \begin{bmatrix} I & & & \\ L_0 & I & & \\ & \ddots & \ddots & \\ & & L_{K-1} & I \end{bmatrix} \begin{bmatrix} F_0 & U_1 & & \\ & F_1 & \ddots & \\ & & \ddots & U_K \\ & & & F_K \end{bmatrix} \qquad (2.11)$$

We then partition the solution vectors $z = (z_0, z_1, \ldots, z_K)$, $x = (x_0, x_1, \ldots, x_K)$, and the right hand side of (2.9) $b = (b_0, b_1, \ldots, b_K)$ according to levels. The matrices $\{F_i\}, i = 0, 1, \ldots, K$ and $\{L_i\}, i = 0, 1, \ldots, K$ can now be obtained

14

using the following recurrence relation:

$$F_0 = A_0$$

$$y_0 = b_0 F_0^{-1}$$

$$\text{for } i = 1 : K$$

$$L_{i-1} = D_{i-1} F_{i-1}^{-1}$$

$$F_i = A_i - L_{i-1} U_i$$

$$y_i = (b_i - y_{i-1} U_i) F_i^{-1}$$

$$\text{end}$$

By backward substitution, one can then find $z_k, k = 0, 1, \ldots, K$:

$$z_K = y_K$$

$$\text{for } i = K - 1 : 0$$

$$z_i = y_i - z_{i+1} L_i$$

$$\text{end}$$

Once z_ks are computed, one can find the steady-state solution to (2.7) by using the identity (2.10).

The block LU factorization algorithm is known to be stable for block tridiagonal matrices that are block diagonally dominant [32]. For the block tridiagonal matrix P, the block diagonal dominance condition is (see [32]):

$$||A_i^{-1}||_1 \geq (||U_i||_1 + ||D_i||_1), \ 0 \leq i \leq K, \tag{2.12}$$

where U_0 and D_K are taken as zero matrices and the 1-norm is defined as the maximum row sum. It can then be checked that the matrix P is block diagonal dominant with the two sides of (2.12) being equal for all i, $0 \leq i \leq K$. Therefore the algorithm is numerically stable ensuring that $\{F_i\}$ and $\{L_i\}$ will not grow without bounds for large i. Note that bulk of the computational effort is concentrated on the LU decomposition of the matrices $\{F_i\}$ required in solving the

15

linear systems in the block-LU decomposition algorithm and the size of F_i equals $i + 1$ for $i \leq W$ and it is $W + 1$ otherwise. Recalling that an LU decomposition requires $2/3N^3$ flops for an $N \times N$ matrix, the proposed algorithm requires $2/3(W + 1)^2(W^2/4 + (W + 1)(K - W + 1))$ flops for all the LU decompositions which in turn gives rise to significant runtime and storage gains compared to the brute force approach.

We note that a new optical packet is blocked under the following two conditions upon the packet's arrival:

- the Markov chain resides in $(K, j), 0 \leq j \leq W$ (i.e. all wavelength channels are in use)

- the Markov chain resides in state $(i, W), W \leq i < K$ (i.e. all converters are in use) and the incoming wavelength is occupied (this occurs with probability i/K)

The PASTA (Poisson Arrivals See Time Averages) property suggests that the steady-state probabilities at arbitrary times as calculated above are the same as those of the embedded discrete-time Markov chain at the epochs of arrivals [28]. Therefore, the packet blocking probability P_b can be expressed as

$$P_b = x_K e + \sum_{i=W}^{K-1} \frac{i}{K} x_{i,W} \tag{2.13}$$

where the solution vector for level i, namely x_i, is partitioned as $x_i = (x_{i,0}, x_{i,1}, \ldots, x_{i,W})$ for $i \geq W$.

2.2 SPL Analysis for Markovian Arrival Process

In this section, we aim at studying the impact of the packet arrival process characteristics on the packet blocking performance. In doing so, we generalize our analytical model of Section 2.1 so as to cover also the MAP (Markovian Arrival Process) arrivals. The MAP generalizes the Poisson process by allowing non-exponential interarrival times but still maintaining its Markovian structure. The MAP is described by two processes, namely the count process $N(t)$ and the phase process $J(t)$, assuming values in $\{0, 1, \ldots\}$ and $\{0, 1, \ldots, m - 1\}$, respectively. The two-dimensional Markov process $\{N(t), J(t)\}$ is then modelled as a Markov process on the state-space $\{(i, j) : i \in \mathcal{Z}, 0 \leq j \leq m - 1\}$ whose infinitesimal generator matrix Q can be represented in block form as

$$
Q = \begin{bmatrix} C & D & & \cdots \\ & C & D & & \cdots \\ & & C & D & \cdots \\ & & & & \ddots \end{bmatrix}.
\tag{2.14}
$$

In the above generator, C and D are $m \times m$ matrices, C has negative diagonal elements and non-negative off-diagonal elements, D is non-negative, and $E = C + D$ is an irreducible infinitesimal generator. When the generator is of the form (2.14) then the underlying process is called MAP which is characterized by the matrix pair (C, D). The evolution of the MAP is as follows. Assume that the Markov process with generator E is in state j, $0 \leq j \leq m - 1$. After an exponentially distributed time interval with parameter $-C_{jj}$, there occurs either a transition to another state $k \neq j$ without an arrival with probability $\frac{C_{jk}}{-C_{jj}}$ or to a state l (possibly the same state) with an arrival with probability $\frac{D_{jl}}{-C_{jj}}$. Let π be the stationary probability vector of the phase process with generator E so that π satisfies

$$
\pi E = 0, \ \pi e = 1
\tag{2.15}
$$

The mean arrival rate λ for a MAP is given by [14]

$$\lambda = \pi D e \qquad (2.16)$$

A subcase of MAP is PH-type which is widely used in the literature for modelling independent and identically distributed but non-exponential interarrival times [33]. To describe a PH-type distribution, we define a Markov process on the states $\{0, 1, \ldots, m\}$ with initial probability vector $(v, 0)$ and an infinitesimal generator

$$\begin{bmatrix} T & t \\ 0 & 0 \end{bmatrix}$$

where v is a row vector of size m, the subgenerator T is an $m \times m$ matrix, and t is a column vector of size m. The distribution of the time till absorption into the absorbing state m is called a PH distribution with representation (v, T). If the interarrival times are modelled by PH distributions, then the arrival process is called a PH-type process. A PH-type process with representation (v, T) is also a MAP by setting $C = T$ and $D = tv$.

Let us now study the optical packet switched link with an arrival process modeled as a MAP with the characterizing pair of two $m \times m$ matrices (C, D). It can be shown that the process $X(t) = \{(i(t), l(t), j(t)) : t \geq 0 \}$ on the state space $S = \{(i, l, j) : 0 \leq i \leq K, 0 \leq l \leq m - 1, 0 \leq j \leq min(i, W)\}$, where $i(t)$ and $j(t)$ are defined as before and $l(t)$ is the phase of the MAP at time t, is also a CTMC. We enumerate the states as $S =$

$$\{\underbrace{(0,0,0), \cdots, (0, m-1, 0)}_{\text{level } 0},$$
$$\underbrace{(1,0,0), (1,0,1), (1,1,0), \cdots, (1, m-1, 1)}_{\text{level } 1}, \cdots$$
$$\underbrace{(K,0,0), \cdots, (K,0,W), (K,1,0), \cdots, (K, m-1, W)}_{\text{level } K}\}$$

$$(2.17)$$

As before, we partition the solution vector $x = (x_0, x_1, \ldots, x_K)$ according to levels. The resulting process can be shown to have an infinitesimal generator of the same block tridiagonal form (2.3) where

$$U_i = D \otimes \bar{U}_i \tag{2.18}$$

$$D_i = \mu I_m \otimes \bar{D}_i \tag{2.19}$$

and

$$A_i = \begin{cases} (C - i\mu I_m) \otimes I_{i+1} & i < W, \\ (C - i\mu I_m) \otimes I_{W+1} + D \otimes \bar{I}_i & W \leq i < K, \\ (E - i\mu I_m) \otimes I_{W+1} & i = K \end{cases} \tag{2.20}$$

where $\otimes$ stands for the Kronecker product and the Kronecker product of an $m \times n$ matrix $A = \{a_{ij}\}$ and a $p \times q$ matrix B is an $mp \times nq$ matrix:

$$A \otimes B = \begin{bmatrix} a_{11}B & \cdots & a_{1n}B \\ \vdots & \cdots & \vdots \\ a_{m1}B & \cdots & a_{mn}B \end{bmatrix}$$

The steady-state probabilities of this CTMC can then be obtained using the same block LU factorization algorithm described in Section 2.1. The PASTA property does not hold since the arrival process is not Poisson. However, by using the arguments in [33], the blocking probability upon a packet arrival can be calculated. In order to do so, we first define the following two matrices

$$G_1 = De \otimes \begin{bmatrix} 1 \\ \vdots \\ 1 \\ 1 \end{bmatrix}, \ G_2 = I_m \otimes \begin{bmatrix} 0 \\ \vdots \\ 0 \\ 1 \end{bmatrix}$$

The packet blocking probability P_b can then be expressed as

$$P_b = \frac{x_K G_1 + \sum_{i=W}^{K-1} \frac{i}{K} x_i G_2 De}{\pi De} \tag{2.21}$$

The above analysis applies to $0 < W < K$. The special cases of $W = 0$ and $W = K$ are studied next.

19

2.2.1 No Wavelength Conversion

In case of NWC (i.e., $W = 0$), we have K independent servers each fed with a MAP that is obtained by splitting the aggregate MAP stream (C, D) evenly into K substreams. The characterizing pair of matrices (C_{NWC}, D_{NWC}) for each substream is given by

$$C_{NWC} = C + \frac{K-1}{K}D, \ D_{NWC} = \frac{1}{K}D$$

The infinitesimal generator for the underlying $MAP/M/1/1$ system for each wavelength channel is then written as

$$Q = \begin{bmatrix} C_{NWC} & D_{NWC} \\ \mu I_m & E - \mu I_m \end{bmatrix} \tag{2.22}$$

Solving the steady state probabilities for (2.22)

$$xQ = 0, xe = 1, x = (x_0, x_1)$$

the blocking probability for each channel is written as

$$P_b = \frac{x_1 D_{NWC} e}{\pi D_{NWC} e} \tag{2.23}$$

2.2.2 Full Wavelength Conversion

The other boundary at $W = K$ is the full wavelength conversion case and the loss system then gives rise to $MAP/M/K/K$ queue. This process has the infinitesimal generator of the form (2.3) where

$$
\begin{aligned}
D_i &= (i+1)\mu I_m, \ 0 \leq i < K \\
A_i &= C - i\mu I_m, \ 0 \leq i < K, \ A_K = E - K\mu I_m \\
U_i &= D, \ 1 \leq i \leq K
\end{aligned}
$$

Solving for the steady-state probabilities of this CTMC and partitioning the solution as $x = (x_0, x_1, \ldots, x_K)$, the blocking probability for the $MAP/M/K/K$ system is given by

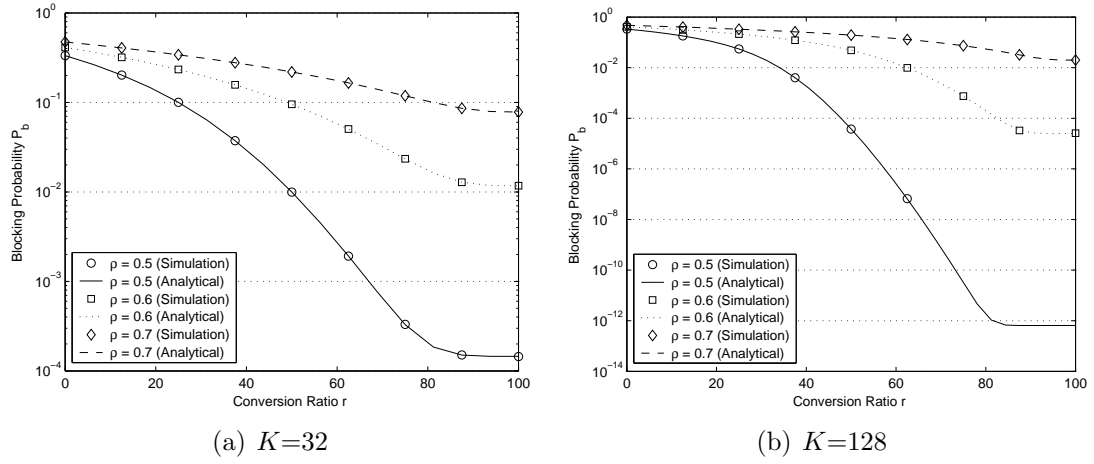|	
(a) K=32	(b) K=128

Figure 2.1: Blocking probability P_b as a function of the wavelength conversion ratio r for three different values of the system load ρ

$$P_b = \frac{x_K De}{\pi De} \tag{2.24}$$

2.3 Numerical Results

The exact analysis method introduced in this thesis for calculating the blocking probabilities in packet switching nodes is implemented using Matlab 6.5. Without loss of generality, we set the mean packet length $1/\mu$ to unity in all the numerical examples.

We first assume that the packet arrival process is Poisson. Using the expression (2.13), the packet blocking probabilities are analytically calculated for the two cases $K = 32$ and $K = 128$ as a function of the wavelength conversion ratio $r := W/K$ and for three different loads $\rho = 0.5, 0.6$, and 0.7, and the results are compared against simulations. We present our results in Fig. 2.1. For all the tested cases, the analytical results are in perfect accordance with the simulation results, validating the proposed approach for Poisson traffic. We note that simulations are not performed in cases where rare probabilities such as $P_b < 10^{-8}$ need to be simulated due to excessive simulation run-times that would be needed.

21

In the second example, we plot the blocking probability P_b as a function of r and ρ in Fig. 2.2 in the form of a 3-dimensional mesh for three different cases of $K = 64$, 128, and 256, respectively. This plot shows that we can obtain blocking probabilities for very large systems (e.g., $K = 256$) and for very rare probabilities (e.g., $P_b \approx 10^{-40}$) and for a wide range of system parameters (i.e., $0.4 < \rho < 1, 0 < r < 1$) without encountering any numerical problems. Moreover, such probabilities can be obtained rather rapidly. Plotting the three planes on Fig. 2.2 required solution of 4554 problems described in Section 2.1 and obtaining Fig. 2.2 consisting of three planes took less than 1 1/2 hours on a 3GHz Pentium based PC. We believe that rapid generation of these plots can be very helpful for converter provisioning purposes as will be described later in the sequel.

The computation times for the case $K = 128$ and $\rho = 0.5$ are plotted in Fig. 2.3(a) as a function of the number of converters W. We observe a faster than linear growth in the execution times when W is small followed by an almost linear behavior in execution times for a wide range of W. The execution times tend to grow slower than linear when W approaches K. The conclusion we draw from this observation is that growth in the size of the converter bank does not pose computational problems as they would in algorithms with polynomial complexity. For the dual case with $W = 80$ and $q = 64$, we observe that the computation times tend to be linear in K as depicted in Fig. 2.3(b).

2.3.1 Effect of Packet Interarrival Time Distribution

We assume that the packet arrival process is phase type and we study the impact of the Coefficient of Variation (CoV) γ of packet interarrival times on packet blocking performance [34]. The CoV of a random variable is the standard deviation divided by the mean of that random variable and is indicative of its variability. For Poisson arrivals $\gamma = 1$, whereas for $\gamma < 1$ we use the Erlang-k distribution which has $\gamma = 1/k$ and which has k phases. On the other hand, the cases of $\gamma > 1$
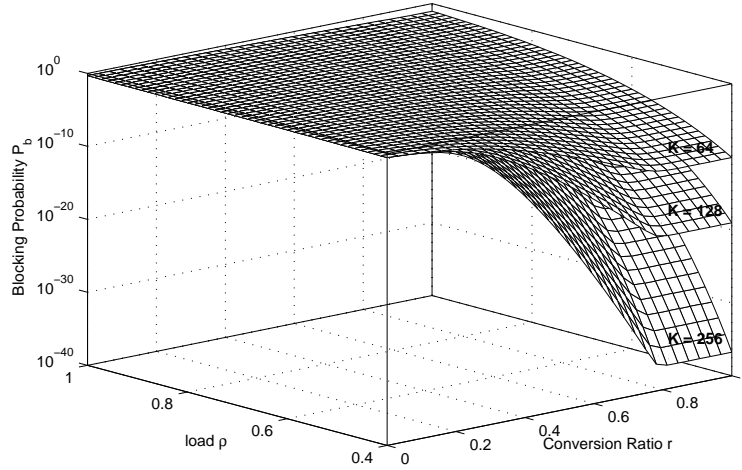
Figure 2.2: Blocking probability P_b as a function of the wavelength conversion ratio r and system load ρ for three different values of K

can be obtained by using an appropriate 2-phase hyper-exponential distribution (denoted by H_2) with balanced means [34]. Fig. 2.4 depicts the packet blocking probabilities as a function of the wavelength conversion ratio for $K = 64$, under two different loads and for different values of the CoV of the arrival process. Again for the PH-type case, we obtain a perfect match of the analytical results with those obtained using simulations. We conclude that packet blocking probabilities are significantly lower for regularly spaced arrivals with relatively small coefficient of variation. This observation demonstrates that not only the mean but also the variance of packet interarrival times have a substantial impact on packet blocking performance and these second order traffic characteristics need to be taken into consideration for accurately modelling optical packet switching systems. We also conclude that traffic shaping at the ingress of an OPS network that can reduce the CoV would also be effective in reducing packet blocking inside the OPS core.

23
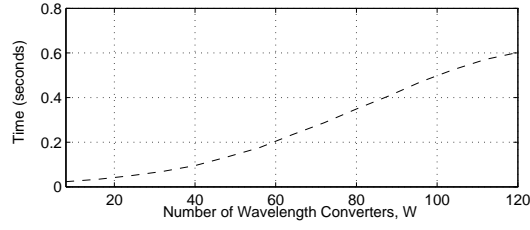
(a)
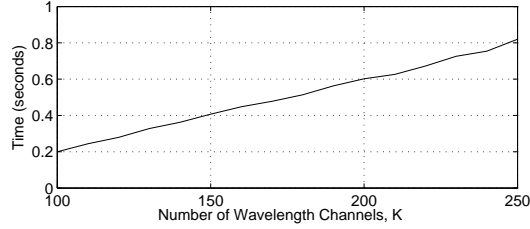
(b)

Figure 2.3: Computation times for (a) with respect to varying W for $K = 128$ (b) with respect to varying K when $W = 80$

2.3.2 Effect of Packet Length Distribution

It is also interesting to study whether the blocking probabilities are sensitive to the packet length distribution. Recall that in the Erlang loss systems, the service time distribution influences the blocking probability only through its mean, and the higher-order statistics does not affect the blocking probabilities. Since the boundary cases of $W = 0$ and $W = K$ reduce to Erlang loss systems of some form, one might lead to the conclusion that the blocking probabilities in the general PWC case, i.e., $0 < W < K$, is also insensitive to the higher order statistics of the packet length distribution. To study this phenomenon, we take three packet length distributions (exponential, deterministic, hyper-exponential) all with the same unity mean but with different CoV values. We then fix $K = 32$, and for different values of W and ρ we obtain P_b but we resort to simulations for non-exponential packet length distributions. The results are presented in Table 2.1. We observe that the blocking probabilities for the PWC system with deterministic and hyper-exponential packet lengths deviate slightly from the one

(a) $\rho = 0.4$

(b) $\rho = 0.6$
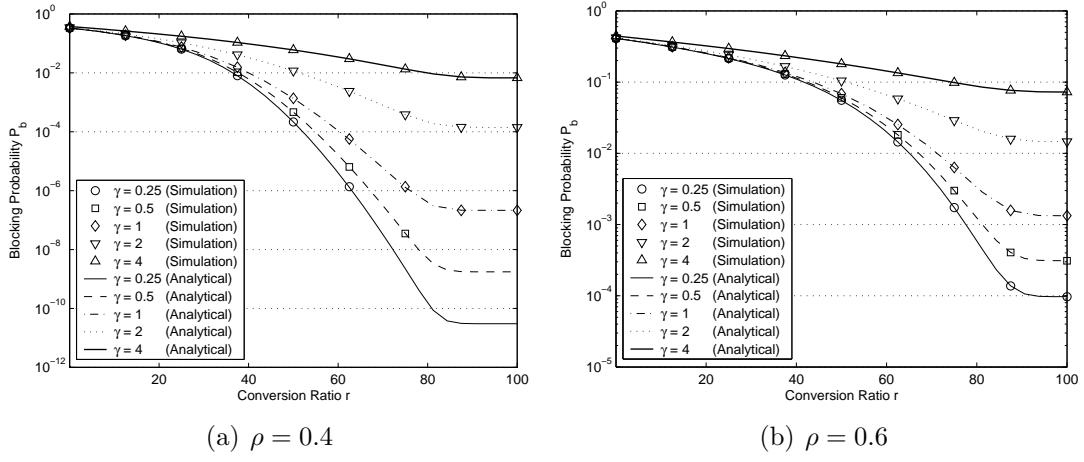
Figure 2.4: Blocking probability P_b for $K = 64$ as a function of r for different values of the coefficient of variation γ

with exponential packet lengths especially under the regime of low load and moderate number of TWCs. These results lead us to believe that the corresponding insensitivity may not be perfect for PWC as in the Erlang loss systems but one can still make use of exponential packet length distributions for approximating the behavior of non-exponential burst lengths.

W	CoV=1	CoV=0 (%95 Conf. Intervals)	CoV=4 (%95 Conf. Intervals)
		$\rho = 0.4$	
4	1.32E-01	1.33E-01 ($\pm$ 3.38E-05)	1.31E-01 ($\pm$ 6.82E-05)
12	7.37E-03	8.14E-03 ($\pm$ 1.39E-05)	7.01E-03 ($\pm$ 2.27E-05)
20	6.76E-05	8.97E-05 ($\pm$ 1.39E-06)	5.59E-05 ($\pm$ 1.22E-06)
28	2.86E-06	2.95E-06 ($\pm$ 2.89E-07)	2.82E-06 ($\pm$ 1.27E-07)
		$\rho = 0.6$	
4	2.65E-01	2.66E-01 ($\pm$ 7.13E-05)	2.65E-01 ($\pm$ 1.05E-04)
12	9.25E-02	9.47E-02 ($\pm$ 8.57E-05)	9.18E-02 ($\pm$ 7.61E-05)
20	1.49E-02	1.65E-02 ($\pm$ 5.18E-05)	1.43E-02 ($\pm$ 3.68E-05)
28	2.17E-03	2.24E-03 ($\pm$ 1.48E-05)	2.12E-03 ($\pm$ 9.25E-06)

Table 2.1: Packet blocking probabilities for exponential, deterministic and hyper-exponential packet length distributions in a number of scenarios

### 2.3.3 Effect of Packet Arrival Process Correlation

Another issue we study is the impact of the arrival process correlation on packet blocking rates. For this purpose, we use the method of [35] which introduces a correlation into an arbitrary uncorrelated arrival process without changing the marginals. As an example if we have a PH-type distribution characterized by the pair (v, T) then the MAP defined by

$$C = T, \; D = (1 - \psi Tev) - \psi T, 0 \leq \psi < 1$$

has a lag-k autocorrelation between the ith and $i + k$th interarrival times in the form $c\psi^k$. A large value of the correlation parameter ψ implies a slow decay of the lag-k autocorrelation function and therefore strong correlation. On the other hand, a small ψ yields weakened autocorrelation and in the limit when $\psi = 0$ we obtain back the uncorrelated phase-type process. As an example, we take an arrival process with hyperexponential marginals with $\gamma = 4$ and we incorporate correlation into this process as described above. In Fig. 2.5, the packet blocking probability is plotted with respect to the correlation parameter ψ in a PWC system with $K = 32$ for two different cases stemming from two different choices of ρ. The results are again in accordance with the simulation results in all cases validating our proposed approach for MAP arrivals. Moreover, increase in the correlation parameter ψ also substantially increases the packet blocking probability as would be expected whereas the impact is more severe with increasing wavelength conversion ratio.
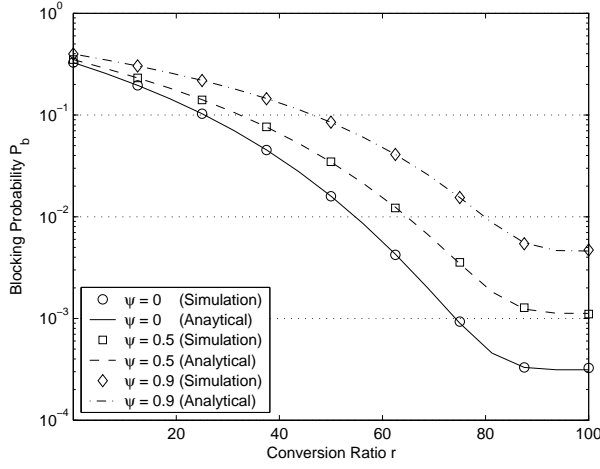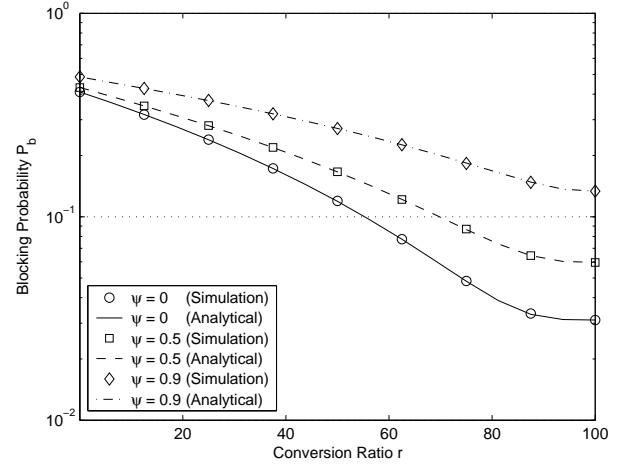
Figure 2.5: P_b for K=32 as a function of the wavelength conversion ratio r for different values of the system load ρ and correlation parameter ψ

Chapter 3

Limited Range Tunable Wavelength Converter Sharing

In this chapter, we try to study Limited Range Wavelength Conversion. We introduce a number of simple-to-implement wavelength conversion policies in Section 3.2. We provide an approximate analysis tool so as to provide a lower bound on the blocking probabilities for the SPL LR-TWC architecture in Section 3.3. The simulation- and analysis-based results are given in Section 3.4. We conclude in the final section.

3.1 Limited Range Wavelength Conversion

In particular, we will study the circular-type limited-range wavelength scheme depicted in Fig. 3.1 in which the Conversion Range (CR) of an incoming wavelength i is given as

$$
CR = \left(\begin{array}{l} \mathrm{mod}(i - \frac{d}{2}, K), \mathrm{mod}(i - \frac{d}{2} + 1, K), \ldots \\ \mathrm{mod}(i + \frac{d}{2} - 1, K), \mathrm{mod}(i + \frac{d}{2}, K) \end{array} \right).
$$
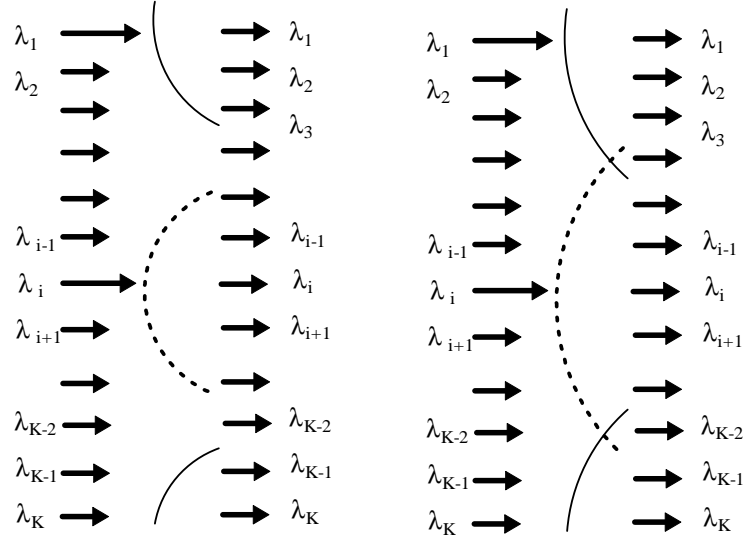
Figure 3.1: The circular conversion scheme depicted for $d = 4$ and $d = 6$ for an edge and a middle wavelength on the fiber link

Circular-type limited-range conversion preserves the symmetry among wavelengths and is therefore the preferred conversion scheme of our work although we believe the results apply to more general and realistic limited-range wavelength conversion schemes.

3.2 Conversion Policies for Limited-Range TWCs

The analysis carried out in Chapter 2 involves FR-TWCs in which a wavelength is selected randomly out of the set of idle wavelengths in case the incoming wavelength is occupied. This randomized policy is best for FR-TWCs when the wavelength of the incoming packets is uniformly distributed. However, such a randomized policy has drawbacks in the case of LR-TWCs even for the case of uniformly distributed wavelengths. We explain this phenomenon by the following scenario. Consider the arrival instance of an optical packet x whose incoming wavelength i is occupied in the outgoing link and therefore the packet requires wavelength conversion. This shows that either a packet had arrived on the same

wavelength i and it is still being served or a packet had arrived on a different wavelength j but converted to i since j was occupied. Since conversions take place within a range of the incoming wavelength, the probability of packet x to find its conversion range fully occupied is larger than the full occupancy probability of an arbitrarily selected set of d wavelengths other than the wavelength i. Equivalently, there is a positive spatial correlation between the status of two neighbouring wavelengths and consequently occupied wavelengths tend to cluster in time as opposed to the case of FR-TWCs. The so-called clustering phenomenon obviously has a detrimental impact on blocking performance. On the other hand, the clustering effect can be reduced by appropriate wavelength conversion policies. We study the following three simple-to-implement wavelength conversion policies at the instance of a packet arrival whose incoming wavelength is occupied.

- *Random Conversion.* The outgoing wavelength is selected randomly from the set of idle wavelengths in the range.

- *Near Conversion* We choose the nearest available wavelength from the set of idle wavelengths in the conversion range and if there exist two such wavelengths, one of them will be selected in random. However, such a policy works in favour of the clustering effect relative to the random conversion policy.

- *Far Conversion.* In this policy, the farthest available wavelength is selected from the set of idle wavelengths in the conversion range. If there exist two such wavelengths, one of them will be selected in random. Obviously, this policy counteracts the clustering effect.

We note that these policies do not affect the steady-state outgoing wavelength distributions because of the symmetry among the wavelengths. Moreover, all three policies obviously result in identical performance for the particular cases

$d = 2$ and $d = K - 1$. In the former case, there are only two adjacent candidate wavelengths for conversion and all three policies collapse to a random conversion policy. The case of $d = K - 1$ reduces to full-range conversion case in which we do not observe clustering. The goal of the simulation study is to show if there is a notable difference among the three conversion policies for $2 < d < K$, i.e. moderate degree of conversion.

3.3   Analytical Model

An exact stochastic analysis for limited range wavelength conversion under the three proposed policies does not appear to be plausible and we will resort to simulations for comparative performance evaluations. However, as a reference we propose the following simple auxiliary model that captures part of the system dynamics. In this model, the conversion range is not the actual $d/2$ neighbourhood of the incoming wavelength but instead a set of arbitrarily selected d wavelengths at each time conversion takes place. This model captures the impact of degree of conversion but does not accommodate the clustering effect. Since the model is cluster-free we conjecture that it provides a lower bound on the blocking probabilities achievable by limited-range wavelength conversion. Moreover, this model is amenable to exact probabilistic analysis based on the procedure in [12]. For the sake of completeness, we present below the exact analysis method for the auxiliary model. In this model, an incoming optical packet

- is forwarded without conversion if its incoming wavelength is idle on the outgoing link

- is directed to the outgoing link after wavelength conversion if there exist both an available TWC and idle wavelength in the conversion range which, in this auxiliary model, is a randomly selected set of d wavelengths other than the incoming wavelength.

- is blocked otherwise

Under the assumptions , let $i(t)$ and $j(t)$ denote the number of wavelength channels and the number of TWCs that are in use at time t, respectively. The process $X(t) = \{(i(t), j(t)) : t \geq 0\}$ is a Continuous Time Markov process on the state space $S = \{(i, j) : 0 \leq i \leq K, 0 \leq j \leq min(i, W)\}$. To show this, let us assume that the process is in some state $(i, j), 0 \leq i < K, 0 \leq j \leq \min(i, W)$ at time t. If a new burst arrives in the interval $(t, t + \delta)$ which occurs with probability $\lambda\delta + o(\delta)$ (i.e., $\lim_{\delta \to 0} o(\delta)/\delta = 0$) [29], there are three possibilities:

A1) the wavelength on which the burst is riding on is not currently used on the link which occurs with probability $(K - i)/K$ and the burst will be admitted and the process will jump to $(i + 1, j)$ at time $t + \delta$,

A2) that wavelength is already used with occurs with probability i/K

- then if $j = W$ then the burst will be blocked because the converter pool is all busy leading to no state change,

- if $j < W$ and all of the wavelength channels that are in conversion range of the riding wavelength are used with probability
$$\frac{\binom{K-d-1}{i-1-d}}{\binom{K-1}{i-1}} \text{ if } i \geq d + 1,$$
the burst will be blocked.

- else the conversion range has at least one free wavelength available then the packet will be admitted on one of the available wavelengths randomly using one of the free converters and the process will make a transition to state $(i + 1, j + 1)$ at time $t + \delta$.

Assume now that the process $X(t)$ is currently in some state $(i, j), 0 < i \leq K, 0 \leq j \leq min(i, W)$ at time t. If a burst departs in the interval $(t, t + \delta)$ which occurs with probability $i\mu\delta + o(\delta)$ then there are two possibilities:

B1) a TWC was used for this burst which occurs with probability j/i and the process $X(t)$ will jump to state $(i-1, j-1)$ at at time $t + \delta$,

B2) a TWC was not used at all for this departing burst which occurs with probability $(i-j)/i$ and the process $X(t)$ will make a transition to state $(i-1, j)$ at time $t + \delta$.

When the process $X(t)$ is in state $(0,0)$, then there cannot be any departures. It is thus clear that the process $X(t)$ is a CTMC and the infinitesimal generator of the CTMC reduces to block-tridiagonal matrix if the states are properly enumerated as in [12]. A numerically stable and efficient solution procedure, the so-called block tridiagonal LU factorization algorithm [31] can then be used to find the stationary solution of the underlying CTMC while taking advantage of the block-tridiagonal structure of the generator.

For obtaining the packet blocking probabilities, we observe that a new packet arrival is blocked if

- the Markov chain resides in $(K, j), 0 \leq j \leq W$ (i.e. all wavelength channels are in use)

- the Markov chain resides in state $(i, W), W \leq i < K$ (i.e. all converters are in use) and the incoming wavelength is occupied (this occurs with probability i/K)

- the Markov chain resides in states $(i, j), d < i < K, 0 \leq j < W$, the incoming wavelength is occupied and the conversion range is fully occupied (this occurs with probability $\frac{i}{K} \frac{\binom{K-d-1}{i-1-d}}{\binom{K-1}{i-1}}$)

By using the PASTA (Poisson Arrivals See Time Averages) property [29], the packet blocking probability P_b of the auxiliary model can be written as

$$P_b = x_K e + \sum_{i=W}^{K-1} x_{i,W} \frac{i}{K} + \sum_{i=d+1}^{K-1} \sum_{j=0}^{W-1} x_{i,j} \frac{i}{K} \frac{\binom{K-d-1}{i-1-d}}{\binom{K-1}{i-1}} \qquad (3.1)$$

33

where $x_i = (x_{i,0}, x_{i,1}, \cdots, x_{i,W})$ for $i \geq W$, $x_{i,j}$ is the steady-state probability of having i wavelengths and j TWCs occupied, and e is column vector of ones.

3.4   Numerical Results

Figure 3.2: Blocking probabilities for $K = 16$ with respect to r for two different values of $\rho = 0.25$ and $\rho = 0.5$ when (a) $d = 2$,(b) $d = 6$,(c) $d = 10$ and (d) $d = 14$

In this study, we obtain the packet blocking probabilities for the three wavelength conversion policies by simulations. We also solve for the auxiliary model analytically using the technique described in the previous section. The goal of this simulation study is to comparatively study the three policies and compare them against the auxiliary model which is clustering-free. Without loss of generality, the mean burst time $1/\mu$ is normalized to unity in all numerical examples
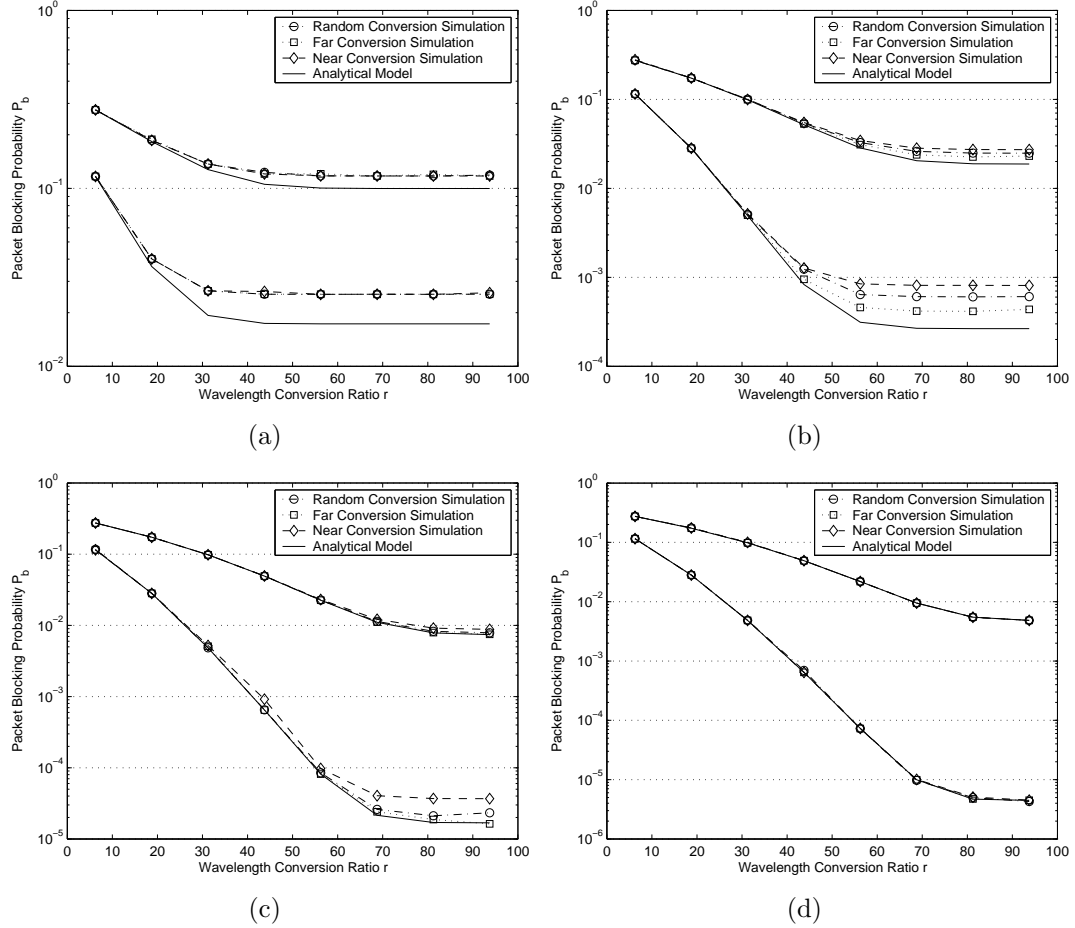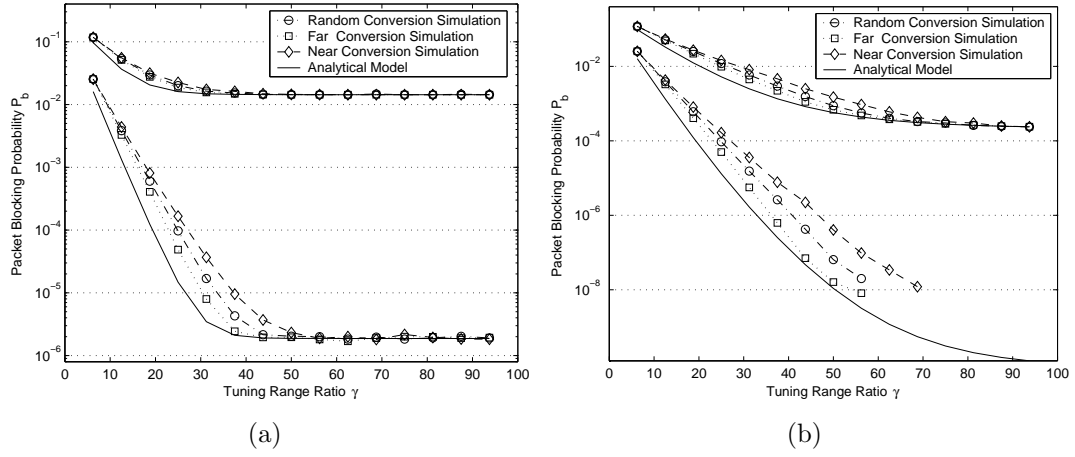
Figure 3.3: Blocking probabilities for $K = 32$ with respect to γ for two different values of $\rho = 0.25$ and $\rho = 0.5$ when (a) $W = 15$ and (b) $W = 25$

presented below. Each simulation result is obtained by averaging 10 independent runs. We do not present blocking probabilities less then 10e-9. We define the system load $\rho = \lambda/\mu K$, wavelength conversion ratio $r = 100\frac{W}{K}$ and tuning range ratio $\gamma = 100\frac{d}{K}$.

In Fig. 3.2, we fix the number of channels K to 16 and we illustrate the packet blocking probabilities with respect to the wavelength conversion ratio r for different values of the tuning range ratio d and for two values of the load ρ. Independent of the conversion policy used, we observe improved utilization of the TWCs with increasing tuning range. We also observe that for small tuning range ratios, it is not as necessary to use large wavelength conversion ratios as in the case of large tuning range ratios. That is because of the fact that the blocking is mostly due to the lack of converters rather than lack of free space in conversion range in small wavelength conversion ratio case. As expected, the three policies provide similar results for both small and large values of d whereas for moderate values of d the "far conversion" policy outperforms the "random conversion" policy which again outperforms the "near conversion" policy. This out-performance is apparent especially for large conversion ratios where the packet losses are mostly due to range occupancy and not the lack of converters. The analytical

model, on the other hand, provides a good approximation only when the tuning range ratio is large but it provides a reference lower bound for all the cases studied.

In the second example, we fix $K = 32$ and investigate the performance of the conversion policies for 4 different pairs of W and ρ values in Fig. 3.3. We note that the impact of "far conversion" policy grows with the increasing K or decreasing ρ, which makes this policy a favorable candidate for next generation dense WDM systems.

Chapter 4

Input Wavelength Conversion in Synchronous Optical Packet Switching

Fig. 4.1 depicts two synchronous broadcast-and-select optical packet switch architectures, referred to as the V1 and V2 architectures, respectively in the E-Photon One Joint Project 1. In V1 (or called NWC), no wavelength conversion is available and in V2 (or called FWC), full wavelength conversion is possible at every input link to reduce contention in output links. Another architecture that is proposed in [10] is the case of PWC where converter sharing is done on a per-input-link basis (i.e., SPIL). However, a wavelength scheduling algorithm is needed to decide on which wavelengths need to be converted so as to minimize the packet loss probability.

In this chapter, we first provide exact blocking probability analysis for the architectures V1 and V2 under asymmetric and symmetric traffic scenarios. We then continue with SPIL architecture, provide an ILP solution and a number of heuristical scheduling algorithms.
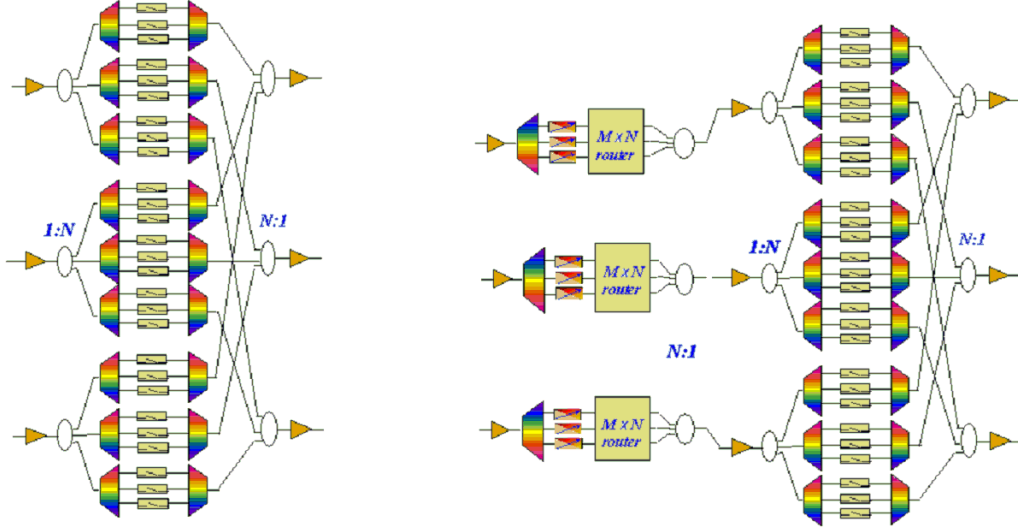
Figure 4.1: Schematic layouts of the V1 (left) and V2 (right) architectures

4.1 Traffic Model

We assume fixed packet sizes and synchronous operation; packet arrival instances are assumed to be aligned to slot boundaries. For V2, we assume full-range wavelength conversion for which an incoming contending wavelength can be converted to any arbitrary wavelength that is free. The traffic distribution is assumed to have a Bernoulli distribution with parameter p; that is in each slot, an input wavelength channel on each link has an optical packet with probability p. The wavelength that a packet is riding on is assumed to be uniformly distributed in the set $(1, 2, \ldots, K)$ where K denotes the number of wavelength channels on each link and N denotes the number of input and output links of the OPS. Based on [10], we define the traffic directivity constant q_l as the probability of directing an incoming packet to the l th outgoing link and we assume that

$$q_i = \frac{1-f}{1-f^N} f^{i-1}, \; i = 1, 2, ..., N$$

Note in particular that the $f = 1$ case corresponds to fully symmetric traffic whereas in the $f = \infty$ case, all incoming traffic is directed to the N th output link (OL), i.e., non-symmetric traffic.

38

4.2 V1 architecture analysis

The packet loss probability for V_1 for the lth OL is given by

$$P_{B_l} = \frac{E\left[\text{Packets lost in outgoing link } l\right]}{E\left[\text{Total number of packets directed to link } l\right]} \quad (4.1)$$

By the Bernoulli distribution of packets and traffic direction probabilities, the denominator can be obtained as

$E\left[\text{Total packets directed to link } l\right]$

$$= K \times \sum_{x=1}^{N} \binom{N}{x} p^x (1-p)^{N-x} \left[\sum_{k=1}^{x} k \binom{x}{k} q_l^k (1-q_l)^{x-k} \right] \quad (4.2)$$

$$= KNpq_l.$$

We note that $k-1$ packets out of k arriving packets on a given wavelength would be lost since we have no wavelength conversion in V1. The numerator of (2) is then expressed as

$E\left[\text{Packets lost in OL } l\right]$

$$= \sum_{x=2}^{N} \binom{N}{x} p^x (1-p)^{N-x} \left[\sum_{k=1}^{N} (k-1) \binom{x}{k} q_l^k (1-q_l)^{x-k} \right]. \quad (4.3)$$

therefore yielding the final blocking probability PV1

$E\left[\text{Packets lost in OL } l\right]$

$$= K \times \sum_{k=2}^{N} (k-1) \binom{N}{k} (pq_l)^k (1-pq_l)^{N-k}, \quad (4.4)$$

39

$$P_{V1} = \sum_{l=1}^{N} q_l P_L$$

$$= \frac{\displaystyle\sum_{l=1}^{N} q_l \sum_{k=2}^{N} (k-1) \binom{N}{k} pq_l^k (1-pq_l)^{N-k}}{Npq_l}. \qquad (4.5)$$

The final blocking probability expression is clearly independent of the number of wavelength channels on a link. It is worthwhile noting that for critical load (i.e., $p = 1$) and symmetric traffic, i.e., $f = 1$ cases, the expression in (4.5) reduces to

$$P_{V1} = \sum_{k=2}^{N} (k-1) \binom{x}{k} \left(\frac{1}{N}\right)^k \left(\frac{N-1}{N}\right)^{N-k} \qquad (4.6)$$

4.2.1   V2 architecture analysis

Using a similar analysis technique as in the V1 architecture, we obtain the following expression for the loss probabilities for V2:

$$P_{V2} = \frac{\displaystyle\sum_{l=1}^{N} q_l \sum_{x=K+1}^{KN} (x-K) \binom{KN}{x} (pq_l)^x (1-pq_l)^{KN-x}}{KNpq_l} \qquad (4.7)$$

The expression above may be computationally hard for large N and K, and we suggest the alternative improved expression below. In this alternative methodology, focusing on the expected number of unblocked packets in contrast with the expected number of blocked packets, we obtain

$$P_{V2} = \sum_{l=1}^{N} \left(q_l - \frac{\left[K + \left[\sum_{x=0}^{K} (x-K) \binom{KN}{x} (pq_l)^x (1-pq_l)^{KN-x} \right] \right]}{KNp} \right).$$

(4.8)

Note that the final expressions for the V1 and V2 architectures can be approximated appropriately for large $KNp(1-p)$ by using the De Moivre - Laplace theorem and by approximating Binomial distributions by Normal distributions. We leave this as a future work. Fig. 4.2 depicts the packet loss probability for the architecture V2 when $K = 8$, as a function of the traffic parameter p, the directivity parameter f, and N.
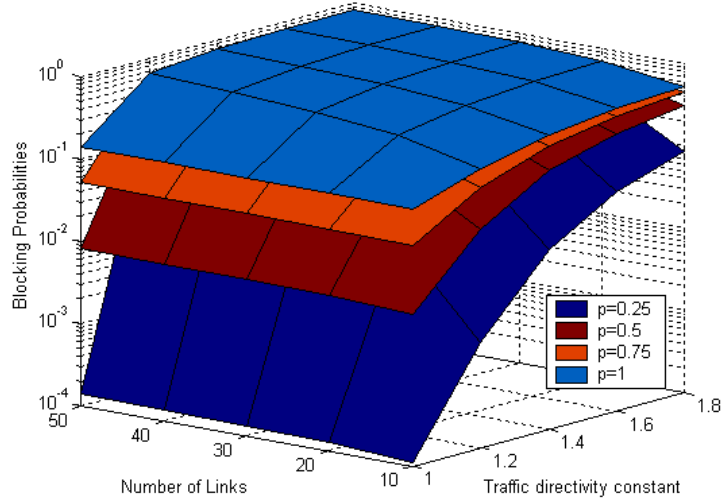
Figure 4.2: Loss probability of the V2 architecture for $K = 8$, varying N and f

The most significant observation from Fig. 4.2 is that the traffic directivity parameter f has an adverse impact on the performance, as expected. Moreover, increasing the number of links slightly increases the loss probability when the number of wavelengths is fixed. In Fig. 4.3, we investigate the throughput gain of the architecture V2 compared to the architecture V1 for $N = 6$, under different scenarios. In Figure Fig. 4.4, we observe that the traffic directivity parameter f

reduces the advantage of using wavelength converters. Using Fig. 4.4, we observe that there exist local maxima points for the relative gain for asymmetric traffic cases unlike the symmetric case for which the throughput gain tends to decrease with increasing system capacity (i.e., K and N) . The second observation is that when the traffic tends to get nonsymmetric, then the throughput gain in using full wavelength conversion decreases. The largest gains are achievable for the symmetric traffic case.

Figure 4.3: Throughput gain of the V2 architecture over V1 for different set of parameters

4.3 Comparison with SPIL Architecture

Another architecture that was proposed in [2] is the case of PWC where converter sharing is done on a per-input-link basis (i.e., SPIL).
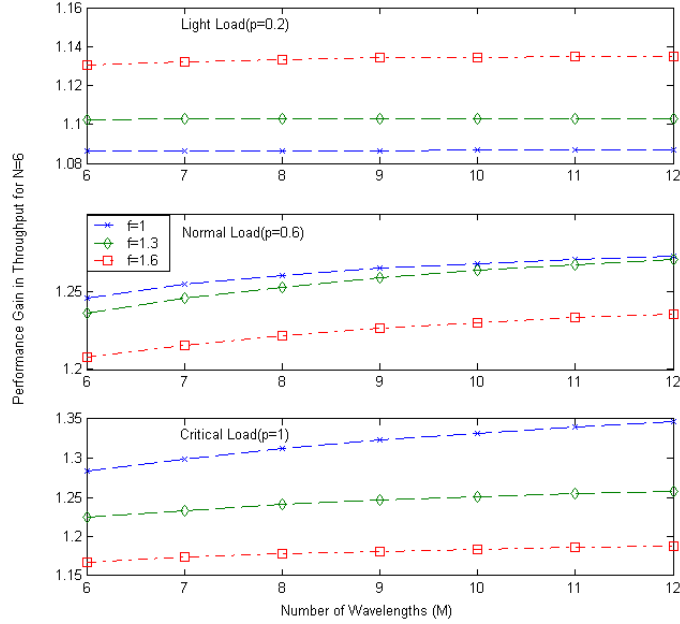
However, a wavelength scheduling algorithm is needed for the SPIL case to determine which wavelengths need to be converted so as to minimize the packet
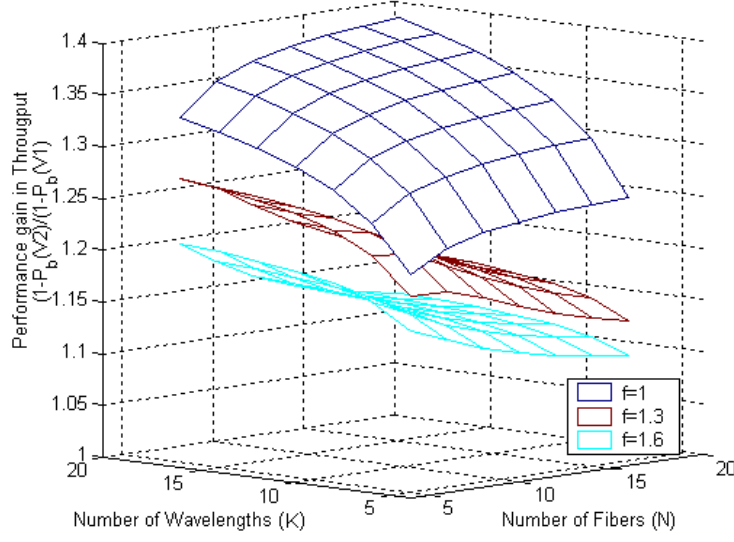
Figure 4.4: Throughput gain of using V2 relative to V1 as a function of K, N, and f

loss probability. We demonstrate the need for such a scheduling algorithm in the following example.

Example. Consider an OPS with two input links (IL), i_1 and i_2, one wavelength converter (WC) dedicated to each IL, and two wavelength channels (WL) per IL, λ_1 and λ_2. Also assume two output links (OL) o_1 and o_2 with one free WL for each; o_1 has λ_2 free and the o_2 has λ_1 free. The notation R_{klw} denotes a packet switching request from the i_k th IL to j_l th OL on wavelength λ_w. Assume that we have the requests R_{111}, R_{122}, R_{222} on the system and the problem is to devise a scheduling mechanism so as to maximize the number of successfully switched packets. If we assign the single WC available to i_1 to R_122 then overall one packet can get transmitted. However, if the WCs for i_1 and i_2 are assigned to requests R_{111} and R_{222}, respectively, then two packets can get transmitted, which actually is the optimal converter assignment policy for this simple scenario. We call the problem of assigning wavelength converters to incoming packet switching requests a "wavelength scheduling" problem for SPIL in this paper. However, the optimal policy is not straightforward to derive in more general scenarios leading

(a) (b)
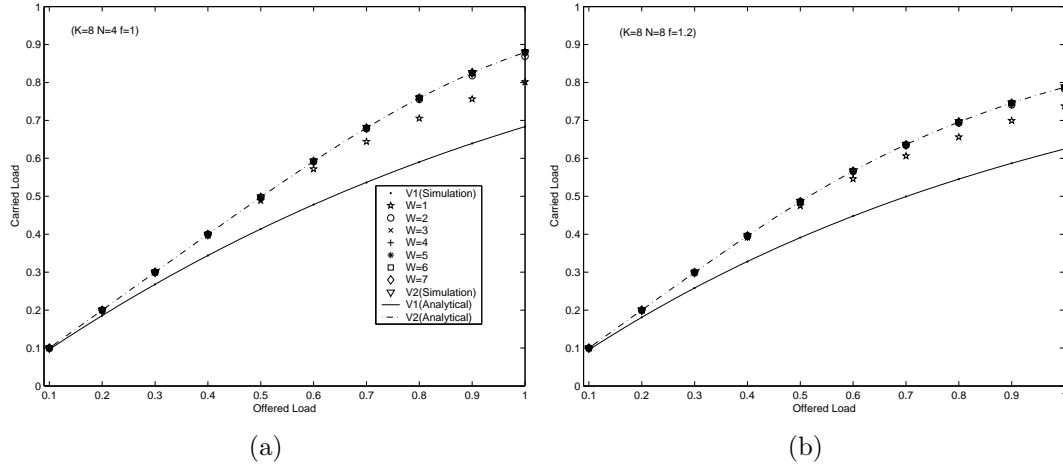
Figure 4.5: Throughput of the evaluated architectures as a function of the offered load and *W* for the cases (a) (*K*=8, *N*=4, *f*=1) and (b) (*K*=8, *N*=8, *f*=1.2)

to a need for intelligent scheduling algorithms for OPSs with SPIL wavelength conversion capability.

The SPIL PWC architecture is illustrated in Fig. 4.6. In the example given, there are three wavelengths per IL and a pool of 2 converters is dedicated for use for that IL.
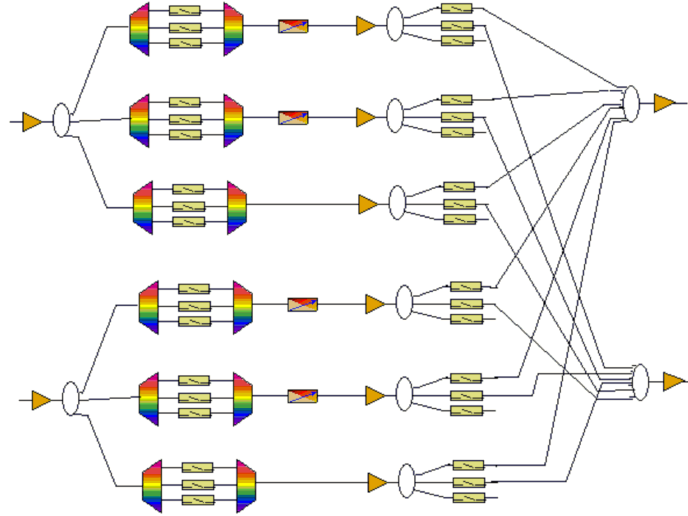
Figure 4.6: Schematic layout of SPIL architecture

Scheduling of SPIL architecture has recently been introduced in [36]. We provide an Integer Linear Programming (ILP) formulation for the SPIL wavelength scheduling problem, however such a method is not amenable to real-time implementation due to computational complexity involved in finding such solutions. Since using ILP solutions are not feasible for real-time implementation, we introduce suboptimal heuristic scheduling algorithms that are amenable to potential real-time implementation in this paper.

Note that for all the wavelength scheduling algorithms discussed below, the assignment of non-contending wavelengths are accomplished without using wavelength converters. As for reducing the complexity of ILP formulation, and for the execution speed of all the heuristic algorithms, we have also applied another rule for contending wavelengths. Since one of the requests for each wavelength group that is destined to a single fiber will be directed without using WCs, we select that unconverted wavelength using a certain algorithm shown in Algorithm 1. This mechanism is used in all algorithms and also in the ILP solution for both reducing the complexity of the problem and for efficient use of WCs efficiently.


Algorithm 1 Pseudo-code for the initial scheduling algorithm that is used for all scheduling mechanisms

---

    for all Incoming Contending Requests **do**
      if an incoming request does not contend for the OL with any other requests
      then
        assign the wavelength to its destined OL.
      else
        continue with the next request.
      end if
    end for
    Form "Contention Groups" by evaluating the destination of the remaining requests.
    Find the number of contending wavelengths in each IL.
    for all the "Contention Groups" **do**
      For each contending group, look for the IL that has maximum number of contentions in each wavelengths.
      Allow the request from IL that has maximum number of contentions to use the OL without contention.
      Update the contention number for the assigned request's IL.
    end for

This algorithm achieves fairly symmetric distribution of contentions among all fibers and therefore allows us to use the WCs efficiently.

4.3.1 The Integer Linear Programming Solution

Since we have assured the allocation of non-converted requests, the ILP formulation now has fewer variables and constraints.. The notation we will use is as follows:

x_{ijw} : The binary variable that indicates request from the w th wavelength channel, whose source is i th IL, and whose destination OL is j th OL and remains as a contending wavelength.

c_i : Number of WCs in the i th IL.

d_j : Number of free WLs on the j th OL.

P : The set of requests which has contention that has not been solved by direct assignment (See the pseudo-code above.)

IS : Denotes the set of ILs

DS : Denotes the set of OLs

WS: Denotes the set of WLs

The ILP formulation presented is as follows:

Maximize

$$\sum_{x \in P} x_{ijw} \tag{4.9}$$

subject to

$$\sum_{j \in DS, w \in WS} x_{ijw} \leqslant c_i, \text{ for all } i . \quad \text{(Converter Constraint)} \qquad (4.10)$$

$$\sum_{i \in IS, w \in WS} x_{ijw} \leqslant d_j, \text{ for all } j . \text{ (Free WL Constraint)} \qquad (4.11)$$

The optimal solution for this problem can now be found by the ILP formulation that maximizes the number of transmitted packets in one slot; however it is not feasible to use in a real- time system. The comparison of the proposed architectures in terms of packet loss probabilities are given in Fig. 4.5 for the symmetric traffic case where WC denotes the size of the converter pool and note that $W = 0$ and $W = K$ cases reduce to the V1 and V2 architectures, respectively.

Studying the loss behavior in Fig. 4.5, we observe that the choice of $W = K/4$ leads to a loss performance very close to that of the FWC architecture for both studied cases. Therefore, one can reduce the cost of wavelength converters by 75% without having to jeopardize the performance of the OPS for the symmetric traffic case. The ILP solution determines the optimal performance that we can achieve from the SPIL architecture, and will be used to evaluate the performance of the scheduling algorithms that we will present hereafter.

4.3.2   Heuristic Scheduling Algorithms

Cost Based Heuristic Algorithms

For achieving the maximum performance from the SPIL-based OPS, we propose to use step by step algorithms that are based on assigning cost values for each request. The general algorithm presented in the Algorithm 1 is used for each of the three cost heuristic algorithms.

Algorithm 2 Pseudo-code for Cost Based Scheduling Algorithms
---
for all the Unscheduled Contending Requests(UCR) **do**
  Determine the cost of each request using the contention parameters available
  if (Minimum Cost $< \infty$) **then**
    Take the request associated with Minimum Cost and accomplish its scheduling. Update the contention parameters and number of used WC's
    .
  else
    Terminate the algorithm and consider the remaining requests as blocked.
  end if
end for

The contention parameters in Algorithm 2 are the number of contending requests from each IL, number of free WLs at the OL, and the number of idle converters at the IL. Below we propose two cost functions:

$$C_1(x_{ijw}) = [\text{FreeWLs[j]} \times \text{Converters[i]}]^{-1} \tag{4.12}$$

$$C_2(x_{ijw}) = \left[\frac{\text{Free WLs[j]} \times \text{Converters[i]}}{\text{Contending[i]}} \right]^{-1} \tag{4.13}$$

We will show that these proposed cost-based algorithms achieve almost the same performance with the ILP solution, albeit the regular cost-update brings significant load to the scheduler. We will denote the cost based algorithms Heuristic I and Heuristic II, respectively.

Link Selection Based Heuristic Algorithms

In need of evading regular cost updates, we also investigated less complex algorithms. The pseudo-code for the two algorithms, which are based on intelligent IL selection and random IL selection, is presented in Algorithm 3.

In the Intelligent Link Selection algorithm, the cost function is

---
Algorithm 3 Pseudo Code for Link Selection Based Algorithms
---
  while $RemainingIL's > 0$ **do**
    Obtain an IL by using a cost function,
    decrease RemainingIL's by one.
    while $MinimumCost < \infty$ AND $Converters[IL] > 0$ **do**
      Assign costs for each UCR by evaluating (1/FreeWLs[OL])
      Accomplish its scheduling
      Update Converters[IL] and FreeWLs[OL] in source IL and destination OL.
    end while
  end while

$$C_3(IL_i\ ) = \ [\text{Contending[i]}]^{-1} \tag{4.14}$$

Since our observations suggested that the ILs with minimum contending requests must be accomplished beforehand, as there will always be blocking in the maximum contending ILs due to the lack of WCs. In the Random Link Selection algorithm, each input link is assigned a random cost before the decision step. These two algorithms will be referred to as Heuristics III and IV respectively.

Random Scheduling Algorithm

The pseudocode for Random Scheduling Algorithm is given in Algorithm 4.

Algorithm 4 Pseudo-Code Random Scheduling Algorithm
---
  while Remaining Contentions > 0 **do**
    Choose an arbitrary request from Remaining Contending Requests
    if (Converters[IL] > 0 AND FreeWLs[OL] > 0 AND Contending[IL] > 0)
    then
      Accomplish the scheduling
      Decrease Converters[IL], FreeWLs[OL] Contending[IL] by one
    end if
    Decrease Remaining Contentions by one, remove the request from the list
  end while

The algorithm will be referred to in the sequel as Heuristic V.

4.4 Numerical Results for Heuristical Scheduling Algorithms

In this section we study the performance of the proposed scheduling algorithms for the case $K = 8$, $N = 8$, $W = 1$, $f = 1$ and $K = 8$, $N = 8$, $W = 2$, $f = 1$. We present our simulation results using the five heuristic algorithms in Tables 4.1-4.2 as well the scheduler obtained through the ILP formulation for the average loss probabilities. We observe that Heuristic I outperforms other heuristics in terms of loss probability. Moreover, results obtained via Heuristic I are very close to those obtained by the ILP solver. When Table 4.2 is analyzed, we note that ILP solution obtains better performance results compared to proposed algorithms with the increasing number of converters, nevertheless proposed algorithms may still be used without significant loss of performance.

Load	ILP	Heur I	Heur II	Heur III	Heur IV	Heur V
0.1	9.37E-06	9.37E-06	9.37E-06	9.37E-06	1.25E-05	6.18E-04
0.2	2.69E-04	2.69E-04	2.69E-04	2.69E-04	3.70E-04	4.76E-03
0.3	2.20E-03	2.20E-03	2.20E-03	2.20E-03	3.15E-03	1.49E-02
0.4	9.78E-03	9.79E-03	9.78E-03	9.79E-03	1.41E-02	3.30E-02
0.5	2.72E-02	2.73E-02	2.72E-02	2.73E-02	3.86E-02	5.84E-02
0.6	5.73E-02	5.77E-02	5.73E-02	5.75E-02	7.68E-02	9.11E-02
0.7	9.60E-02	9.68E-02	9.61E-02	9.64E-02	1.20E-01	1.28E-01
0.8	1.39E-01	1.40E-01	1.39E-01	1.39E-01	1.63E-01	1.68E-01
0.9	1.81E-01	1.82E-01	1.81E-01	1.82E-01	2.03E-01	2.08E-01
1	2.21E-01	2.22E-01	2.21E-01	2.21E-01	2.41E-01	2.48E-01

Table 4.1: Blocking Probabilities for K=8, N=8 , W=1, f=1.

Load	ILP	Heur I	Heur II	Heur III	Heur IV	Heur V
0.1	——	——	——	——	——	——
0.2	——	——	——	——	——	——
0.3	——	——	——	——	——	1.08E-03
0.4	1.17E-03	1.17E-03	1.17E-03	1.17E-03	1.17E-03	5.08E-03
0.5	6.54E-03	6.54E-03	6.54E-03	6.54E-03	6.54E-03	1.46E-02
0.6	1.94E-02	1.94E-02	1.94E-02	1.94E-02	2.02E-02	3.94E-02
0.7	4.08E-02	4.13E-02	4.08E-02	4.08E-02	4.28E-02	6.52E-02
0.8	6.84E-02	6.94E-02	6.86E-02	6.88E-02	7.27E-02	9.29E-02
0.9	9.72E-02	1.00E-01	9.80E-02	9.94E-02	1.03E-01	1.31E-01
1	1.43E-01	1.47E-01	1.45E-01	1.46E-01	1.51E-01	1.77E-01

Table 4.2: Blocking Probabilities for $K=8$, $N=8$, $W=2$, $f=1$.

Chapter 5

CONCLUSION

In this thesis, we analyzed an exact analytical method for exactly calculating blocking probabilities in OPS/OBS nodes employing shared wavelength conversion. The method is first formulated for Poisson arrivals and then extended to the more general Markovian arrivals which are used for traffic modeling in the Internet. This exact analysis method can be used for efficiently calculating blocking probabilities even in very large systems with hundreds of wavelength channels and very rare blocking probabilities. Rapid calculation of the packet blocking probabilities is shown to be crucial in provisioning bufferless OPS links when the cost relationship between a wavelength channel and a wavelength converter is available. Moreover, we show that the variability of the interarrival times and the correlation structure also impact the blocking probabilities in asynchronous optical packet switching systems and such second-order statistics also need to be taken into account.

We also studied the performance of asynchronous optical packet switching architectures equipped with a number of limited-range tunable wavelength converters shared on a per-output-link basis. We identified the wavelength clustering effect to describe the spatial correlation among the occupied wavelengths which

is detrimental to blocking performance in systems with limited-range converters. We proposed a "far conversion" policy to reduce the clustering effect and we showed through simulations that this proposed policy substantially outperforms "random" and "near" conversion policies especially in the low load and moderate tuning range ratio regimes, We also introduced a Markovian auxiliary model that captures the effect of the tuning range but not the clustering phenomenon, in order to provide a lower bound on the blocking probabilities for the three studied wavelength conversion policies.

Finally, in this thesis we investigated the performance of optical packet switching with input wavelength conversion. Analytical methods for full conversion and no conversion cases are derived for synchronous symmetric and asymmetric traffic scenarios. We investigated the "share-per-input-link" architecture, revealing its potential by obtaining the optimum performance with integer linear programming formulation. We have observed that one can achieve similar performance as full conversion by using partial wavelength conversion considering the analyzed architecture. Moreover, heuristic scheduling algorithms which utilize that potential were also proposed. By simulation studies, we showed that cost-based heuristic scheduling algorithms can achieve close blocking performance as that of the linear programming solution, at the expense of frequent updates. We have also underlined that link selection based heuristical algorithms may be another good alternative due their efficiency in cost updates.

Bibliography

[1] P. Gambini, M. Renaud, C. Guillemot, F. Callegati, I. Andonovic, B. Bostica, D. Chiaroni, G. Corazza, S. L. Danielsen, P. Gravey, P. B. Hansen, M. Henry, C. Janz, A. K. R. Krahenbuhl, C. Raffaelli, M. Schilling, and A. T. L. Zucchelli, "Transparent optical packet switching: Network architecture and demonstrators in the KEOPS project," *JSAC*, vol. 16, no. 7, pp. 1245–1259, 1998.

[2] G. N. Rouskas and L. Xu, "Optical packet switching," in *Optical WDM Networks: Past Lessons and Path Ahead* (K. Sivalingam and S. Subramaniam, eds.), Norwell, Massachusetts: Kluwer, 2004.

[3] C. Qiao and M. Yoo, "Optical burst switching (OBS) - a new paradigm for an optical Internet," *Jour. High Speed Networks (JHSN)*, vol. 8, no. 1, pp. 69–84, 1999.

[4] Y. Chen, C. Qiao, and X. Yu, "Optical burst switching: A new area in optical networking research," *IEEE Network Mag.*, vol. 18, no. 3, pp. 16–23, 2004.

[5] R. A. Barry and P. Humblet, "Models of blocking probability in all-optical networks with and without wavelength changers," *IEEE J. Sel. Areas Commun.*, vol. 14, pp. 858–867, 1996.

[6] E. Karasan and E. Ayanoglu, "Effects of wavelength routing and selection algorithms on wavelength conversion gain in WDM optical networks," *IEEE/ACM Trans. Networking*, vol. 6, no. 2, pp. 186–196, 1998.

[7] M. Kovacevic and A. Acampora, "Benefits of wavelength translation in all-optical clear channel networks," *IEEE J. Sel. Areas Commun.*, vol. 14, pp. 868–880, 1996.

[8] K. Lee and V. Li, "A wavelength convertible optical network," *IEEE Jour. Lightwave Tech.*, vol. 11, pp. 962–70, 1993.

[9] V. Eramo, M. Listanti, and P. Pacifici, "A comparison study on the wavelength converters number needed in synchronous and asynchronous all-optical switching architectures," *IEEE Jour. Lightwave Tech.*, vol. 21, pp. 340–355, 2003.

[10] V. Eramo and M. Listanti, "Input wavelength conversion in optical packet switches," *IEEE Comm. Letters*, vol. 7, no. 6, pp. 281–283, 2003.

[11] V. Puttasubbappa and H. Perros, "An approximate queueing model for limited-range wavelength conversion in an obs switch," in *Networking 2005*, 2005.

[12] N. Akar and E. Karasan, "Exact calculation of blocking probabilities for bufferless optical burst switched links with partial wavelength conversion," in *1st Conference on Broadband Networks (BROADNETS'04), Optical Networking Symposium*, pp. 110–117, 2004.

[13] D. M. Lucantoni, K. S. Meier-Hellstern, and M. F. Neuts, "A single server queue with server vacations and a class of nonrenewal arrival processes," *Adv. Applied Prob.*, vol. 22, pp. 676–705, 1990.

[14] D. M. Lucantoni, "New results for the single server queue with a batch Markovian arrival process," *Stochastic Models*, vol. 7, pp. 1–46, 1991.

[15] M. F. Neuts, *Structured Stochastic Matrices of M/G/1 Type and Their Applications.* Marcel Dekker, N.Y., 1989.

[16] G. Latouche and V. Ramaswami, *Introduction to matrix analytical methods in stochastic modeling.* ASA-SIAM Series on Statistics and Applied Probability, 2002.

[17] A. Kuczura, "The interrupted Poisson process as an overflow process," *Bell Sys. Tech. Jour.*, vol. 52, pp. 437–448, 1973.

[18] A. Riska, V. Diev, and E. Smirni, "Efficient fitting of long-tailed data sets into phase-type distributions," *SIGMETRICS Perform. Eval. Rev.*, vol. 30, no. 3, pp. 6–8, 2002.

[19] H. Heffes and D. Lucantoni, "A Markov modulated characterization of packetized voice and date traffic and related statistical multiplexer performance," *JSAC*, vol. 4, no. 6, pp. 856–868, 1986.

[20] D. P. Heyman and D. Lucantoni, "Modeling multiple IP traffic streams with rate limits," *IEEE/ACM Trans. Netw.*, vol. 11, no. 6, pp. 948–958, 2003.

[21] P. Salvador, R.Valadas, and A. Pacheco, "Multiscale fitting procedure using Markov modulated Poisson processes," *Telecommunication Systems*, vol. 23, no. 1-2, pp. 123–148, 2003.

[22] L. Muscariello, M. Mellia, M. Meo, R. L. Cigno, and M. A. Marsan, "An MMPP-based hierarchical model of Internet traffic," in *ICC*, June 2004.

[23] R. Ramaswami and K. N. Sivarajan, *Optical Networks: A Practical Perspective.* Morgan Kaufmann Publishers, 2 ed., 2002.

[24] D. Mitra, C. Nuzman, I. Saniee, and P. Whiting, "Optical cross-connect with shared wavelength conversion under dynamic load," *IEEE/OFC Technical Digest*, pp. 160–162, 2002.

[25] Y. Mingwu, L. Zengji, and W. Aijun, "Accurate and approximate evaluations of asynchronous tunable-wavelength-converter sharing schemes in optical burst-switched networks," *IEEE Jour. Lightwave Tech.*, vol. 23, no. 10, pp. 2807–2815, 2005.

[26] C. M. Gauger, "Performance of converter pools for contention resolution in optical burst switching," in *SPIE Optical Networking and Communications Conference (OptiComm 2002)*, 2002.

[27] J. Spath and S. Bodamer, "Routing of dynamic Poisson and non-Poisson traffic in WDM networks with limited wavelength conversion," in *24th European Conference on Optical Communication*, 1998.

[28] D. Gross and C. M. Harris, *Fundamentals of Queueing Theory.* Wiley, 3rd ed., 1997.

[29] L. Kleinrock, *Queuing Systems, Vol. 1, Theory.* John Wiley, New York, 1989.

[30] W. J. Stewart, *Introduction to the numerical solution of Markov chains.* Princeton University Press, 1994.

[31] G. H. Golub and C. F. van Loan, *Matrix Computations.* The Johns Hopkins University Press, 3 ed., 1996.

[32] J. Demmel, N. J. Higham, and R. Schreiber, "Block LU factorization," *Numerical Lin. Alg. and Appl.*, vol. 2, no. 2, pp. 173–190, 1995.

[33] M. F. Neuts, *Matrix-geometric solutions in stochastic models.* Baltimore, MD: Johns Hopkins University Press, 1989.

[34] B. R. Haverkort, *Performance of Computer and Communication Systems: A Model-based Approach.* John Wiley and Sons, 1998.

[35] K. Mitchell, "Constructing a correlated sequence of matrix exponentials with invariant first-order properties," *Operations Research Letters*, vol. 28, pp. 27–34, 2001.

[36] V. Eramo, M. Listanti, and A. Valetta, "Scheduling algorithms in optical packet switches with input wavelength conversion," *Computer Communications*, vol. 28, no. 12, pp. 1456–1467, 2005.